RNI: DELENG/2005/15153
Regn No. DL (DS)-112/MP/2026-27-28
Rs.200

ISSN 0973-2136

www.mycoordinates.org

Coordinates

Volume XXII, Issue 07, July 2026

THE MONTHLY MAGAZINE ON POSITIONING, NAVIGATION AND BEYOND

AI FOR ARCHITECTURE

FROM STYLE-DRIVEN GENERATION TO STRUCTURE-GUIDED DESIGN

GNSS (SBAS) Constellation Specific Monthly Analysis Summary: June 2026

In Coordinates

10 years before...

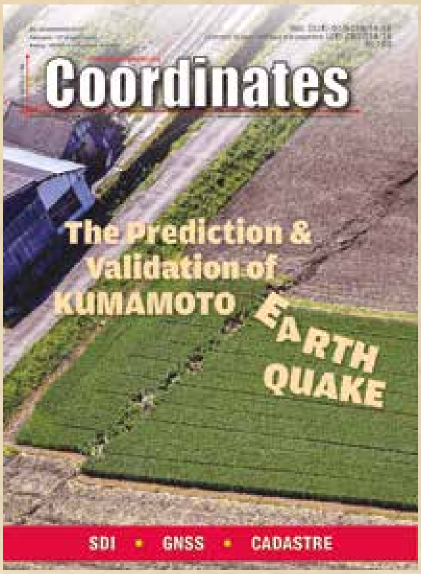

mycoordinates.org/vol-XII-issue-07-July-2016

The Prediction and Validation of Kumamoto Earthquake

Dr Shunji Murai, Professor Emeritus, University of Tokyo and Advisor, Japan Earthquake Science Exploration Agency (JESEA)
Dr Harumi Araki, Director, Environmental Geology Laboratory and Advisor, JESEA

It was very difficult to achieve the prediction of the Kumamoto Earthquake because there were very few short term abnormal changes at multiple GNSS stations which have normally occurred, in our previous experience, for larger earthquakes. Only long term changes of trends in subsidence in the Kyushu area, which have been recognized in the previous two years, would have been the scientific evidence for our predictions.

Mainstreaming Spatial Data Sharing approach in Sri Lanka

Dr Lesley Arnold, Director Geospatial Frameworks, Perth, Western Australia Research Fellow, Department of Spatial Sciences, Curtin University, Western Australia Cooperative Research Centre for Spatial Information

While SDI solutions come with some significant challenges, getting the policy and governance components in place early will allow governments to achieve major incremental steps towards achieving a robust data sharing solution; one in which business leaders, not-for-profit project teams and policy makers can work at scale using the best available data, and where project-level data can be scaled up and reused in the national interest well beyond a project's lifetime. This is the plan for the Sri Lanka SDI.

EGNOS-based Reactive Locator for the European Train Control System

Aleš Filip, Faculty of Electrical Engineering and Informatics, University of Pardubice, Czech Republic

This paper describes a novel train LDS solution based on EGNOS for ETCS. The solution consists in LDS with reactive fail-safety based on EGNOS V2 or EGNOS V3, which is further combined with a newly introduced travelling virtual balise (TVB) concept.

Systematic Cadastre Surveying and Inventory of Real Estate Objects in Azerbaijan

In the frame of the project SCPI, the consultant and involved private companies contributed a lot to establish a sustainable land administration system in Azerbaijan. In the course necessary data was not only collected to register ownership but also for a sustainable Land Management. The Republic of Azerbaijan is on a good way, but there is still a lot to do …

Challenges to Climate Action and Resource Use Efficiency in South Asia

Dr Rishiraj Dutta, Asian Disaster Preparedness Center, Bangkok, Thailand

The study has revealed that there has been considerable impacts from climate change in South Asia. Although countries have been taking initiatives to overcome the impacts of climate change, a lot of work still remains to be done. The study has shown that policies have been in place but the institutional mechanisms needs to be further strengthened to effectively implement the existing policies.

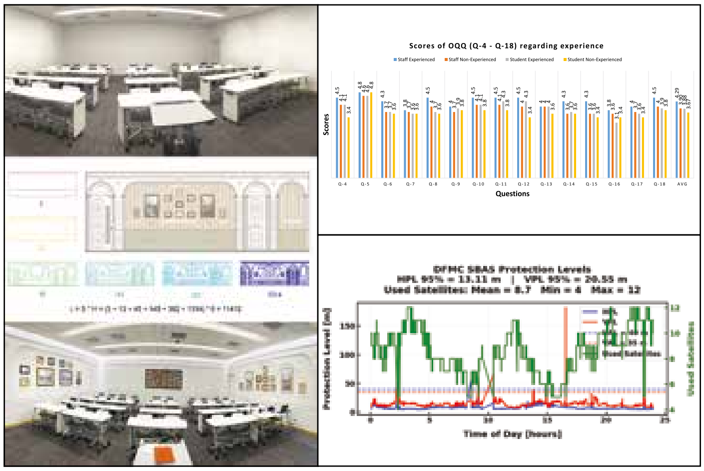

In this issue

Coordinates Volume 22, Issue 07, July 2026

Articles

Columns

This issue has been made possible by the support and good wishes of the following individuals and companies
Aadithya Sujit, Benjamin J. Watkinson, Bin Jiang, Chris Gilbert, Claire Tinker-Mill, Darren Ansell, David Jones, John M. Pinder, Kaya Kuru, Keith Vinning, Lee Moore, Narayan Dhital, and Sam Worthington; SBG System, and many others.

Mailing Address
A 002, Mansara Apartments
C 9, Vasundhara Enclave
Delhi 110 096, India.
Phones +91 11 42153861, 98102 33422, 98107 24567

Email
[information] talktous@mycoordinates.org
[editorial] bal@mycoordinates.org
[advertising] sam@mycoordinates.org
[subscriptions] iwant@mycoordinates.org
Web www.mycoordinates.org

Annual subscription (12 issues)
[India] Rs.1,800* [Overseas] US$100*
*Excluding postage and handling charges

Printed and published by Sanjay Malaviya on behalf of Coordinates Media Pvt Ltd
Published at A 002 Mansara Apartments, Vasundhara Enclave, Delhi 110096, India.
Printed at Hi-Tech Graphics, Okhla Industrial Area 2, New Delhi, India

Editor Bal Krishna
Owner Coordinates Media Pvt Ltd (CMPL)

This issue of Coordinates is of 36 pages, including cover.

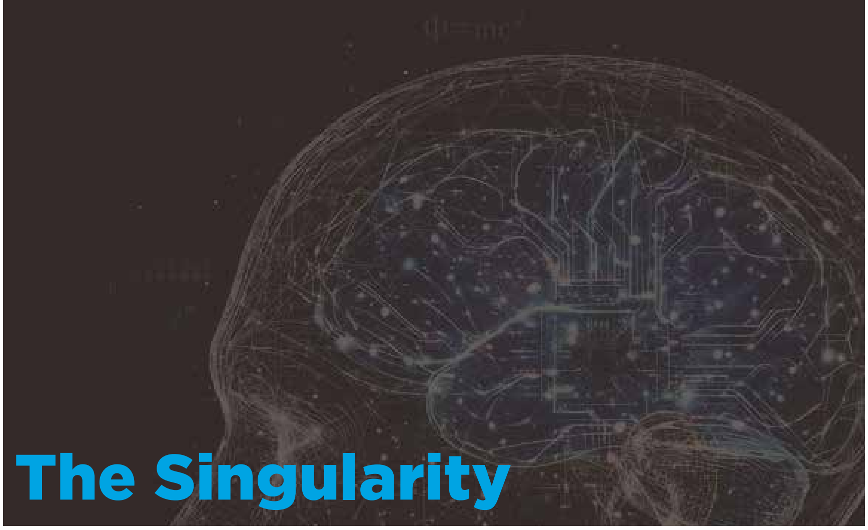

The Singularity

OpenAI's Sam Altman believes that AI has entered the 'singularity',

The point at which AI outpaces human intelligence and becomes difficult to control.

If such a threshold is ever crossed,

Technological progress could accelerate beyond humanity's ability

To predict, regulate, or even fully comprehend.

That possibility explains why some experts advocate

Stronger safeguards, independent oversight, and even emergency "kill switches."

Others insist we are still far from it.

The disagreement is revealing.

The world's most powerful technology is advancing,

Even as its creators differ on where it is heading.

That calls neither for panic nor complacency, but informed vigilance.

The danger is not the arrival of 'singularity',

But humanity sleepwalking into a future it does not understand fully,

Only to become a victim of its own invention.

Bal Krishna, Editor
bal@mycoordinates.org

AI for architecture: From style-driven generation to structure-guided design

AI for architecture, on this account, is less about spectacle than about the quiet, demanding work of structural diagnosis and structurally constrained generation.

Bin Jiang
LivableCityLAB, Urban Governance and Design Thrust, The Hong Kong University of Science and Technology (Guangzhou), China

Abstract

This essay argues that the most consequential question for AI in architecture is not whether AI can generate buildings, but whether it can be guided toward designs that are coherent, beautiful, and supportive of human life. To move past the present impasse of style-driven generation, the essay develops a Living Structure + AI paradigm grounded in Christopher Alexander's theory and operationalised through a skeleton–skin workflow. The skeleton encodes hierarchical order through nested substructures and computable indicators — the L-score and the B-score produced by the Beautimeter; the skin is generated by AI under structural constraint. The paradigm is illustrated through four real renovations on the HKUST(GZ) campus and connected to recent — and still preliminary — results in which large language models, properly prompted, judge architecture in broad agreement with public preference and with measured brain responses. AI for architecture, on this account, is less about spectacle than about the quiet, demanding work of structural diagnosis and structurally constrained generation.

1. Introduction

1.1. The question worth asking

Generative artificial intelligence has entered architecture quickly and ambiguously. Large language models, diffusion-based image synthesis, and multimodal systems are now routine in studios, classrooms, and competition entries (del Campo and Leach, 2022; Leach, 2023). The temptation is to treat AI as a faster way to produce form — a machine for spectacular novelty — and conferences and journals fill with AI-generated facades that look like nothing ever built and, often, like nothing anyone would want to inhabit (Fig. 1).

The most important question is not whether AI can generate designs — that is settled — but whether it can be guided toward designs that are good for people: coherent, beautiful, comfortable, and durable. This moves AI from the periphery of formal experimentation toward an older debate about what buildings and cities ought to be (Alexander, 1979; Mehaffy, 2020; Salingaros, 2006).

Three commitments anchor the argument: that the difference between environments that feel alive and those that do not is real, not merely subjective taste (Alexander, 2002–2005; Salingaros & Sussman, 2020); that it can be described, measured, and partially explained through living structure (Jiang, 2019; Jiang & de Rijke, 2023; LivableCityLAB, 2025); and that AI, properly framed, is less a threat to human-centered design than a powerful ally, provided it is constrained by structural principles rather than turned loose on style alone.

1.2. A discipline at a crossroads

Architectural education has been accused of detaching from lived experience, privileging abstract aesthetics over human reality (Architecture Education Declares, 2019; Curl, 2018), and grassroots movements — New Traditional Architecture, Architectural Uprising, Humanise — have arisen in response (Boys Smith, 2016; Heatherwick, 2023). Governments, meanwhile, are shifting from large-scale construction to long-term, people-centered urban governance and renewal (Gehl, 2010; Mehaffy & Salingaros, 2015; Xinhua News Agency, 2025).

These shifts make the moment both fertile — we now have computational tools to help produce coherent design at scale — and dangerous, since tools deployed without structural grounding will only accelerate the fragmented, image-driven architecture they aim to leave behind.

1.3. What is missing in current AI practice

Yet much of present AI practice in architecture remains, in a meaningful sense, structure-blind. The dominant mode is text-to-image: a designer types a prompt and the model returns a glossy render. The results are visually arresting but, on close inspection, often unbuildable, contextually incoherent, and detached from the deeper principles that distinguish a beloved place from a disliked one. Where AI is used to optimise — for energy performance, circulation, or daylighting — the optimisation typically runs over geometries that have already been chosen on stylistic grounds.

Three patterns recur: *surface fascination,* in which AI is asked almost exclusively to produce skins; an *absence of internal structure,* in which the skeletal organisation behind striking renders is rarely articulated; and a *difficulty of measurement,* in which practitioners struggle to say why one AI-generated design is better than another except by reference to taste.

1.4. The argument in brief

The Living Structure + AI paradigm reframes the situation through four connected claims. First, the tension between structural coherence and stylistic diversity is a false dichotomy: traditional architectures across cultures combine deep hierarchical order with rich surface variation (Alexander et al., 1977; Salingaros, 2006). Second, this can be made operational through a skeleton–skin distinction. Third, AI is best understood not as a generator of arbitrary form but as a structural mediator. Fourth, the reframing bears directly on design education, urban governance, and the assessment of architectural quality.

2. Living structure: A theory of what makes buildings alive

The structural backbone of this essay is the theory of living structure. Articulated by Alexander (2002–2005) in the four-volume *Nature of Order,* the theory begins with a simple observation: environments that feel alive — coherent, welcoming, satisfying — differ from those that do not, and the difference is not arbitrary but can be described, partly explained, and increasingly measured (Jiang, 2025; Jiang & de Rijke, 2023; Salingaros, 2006). Living structure is the order that supports this felt quality, found in nature, vernacular settlements, and well-loved cities (Bak, 1996; Eglash, 1999; Mandelbrot, 1982), and can be deliberately produced — though contemporary practice often obstructs it.

Fig. 1. Two near-identical urban streetscapes — a contemporary scheme (left) and a more traditional, human-scaled alternative (right). Public polls and properly prompted AI judges prefer the latter. The image opens the essay's central question: by what criteria should we ask AI to choose? Adapted from Boys Smith and Salingaros (2025).

2.1. Two faces of the same phenomenon

Living structure has two complementary aspects. Living is the emotional, sensible, right-brain perception of an environment as whole, alive, and resonant with one's own sense of self. Structure is the computable, measurable, left-brain face of the same phenomenon — geometric properties, hierarchical relations, and quantitative indicators. The paradigm developed below rests on bringing the two into systematic correspondence: what the left brain can compute helps us design for what the right brain can feel.

2.2. The fifteen properties, two laws, two principles

Alexander (2002–2005) identified fifteen geometric properties that recur in environments experienced as alive (Fig. 2) — a vocabulary distilled from long observation of vernacular architecture, sacred buildings, urban settlements, and natural systems.

The fifteen are: levels of scale, strong centres, thick boundaries, alternating repetition, positive space, good shape, local symmetries, deep interlock and ambiguity, contrast, gradients, roughness, echoes, the void, simplicity and inner calm, and not-separateness. Together they amount to a generative grammar of life in space.

Two fundamental laws underlie these properties. *The scaling law* (Jiang, 2015) states that any coherent, living whole exhibits far more small substructures than large ones — visible in the branching of rivers, the venation of leaves, and the room sizes within a beloved house. *Tobler's law*

(Tobler, 1970) states that nearby centres or substructures tend to be similar in size and character, giving well-formed environments their characteristic local rhythm.

Two design principles operationalise the laws. *Differentiation* is the process by which an undifferentiated whole is gradually sub-divided into coherent centres at multiple levels of scale. *Adaptation* is the process by which substructures adjust to one another and to context (Alexander, 2002–2005). Together they convert living structure from a descriptive notion into a generative one.

2.3. Quantifying living structure: the L-score and the B-score

The *L-score* (Jiang & de Rijke, 2023) captures the depth and richness of hierarchical substructures. It is defined as $L = S \times H$, where S is the total number of substructures across all levels and H is the depth of the hierarchy. A recursive subdivision yielding $1 + 2 + 8 + 32 = 43$ substructures across four levels gives an L-score of 172. Higher L-scores indicate richer, deeper hierarchy. The L-score makes “far more smalls than larges” concrete: it rewards structures whose finer levels contain many more components than their coarser ones (Fig. 3).

The *B-score*, produced by the Beautimeter (Jiang, 2025), measures the presence of the fifteen properties. By submitting an image to a vision-capable language model under a carefully engineered prompt, the Beautimeter returns an aggregate score between 0 and 15. Validation against the ScenicOrNot dataset of more than 1800 user-generated beauty ratings paired with street-view imagery shows that B-scores correlate with human judgments at a correlation of about 0.62 ($p < 0.01$), with overall pairwise accuracy near 75 percent and order-invariant precision documented in a full confusion matrix (Jiang, 2025; Xue & Jiang, 2026). The model is not trained on human ratings but is prompted on geometric properties and then validated against independent human ratings — and, separately, against the behavioural and neural outcomes reported below (Yin et al., 2026) — so the agreement is a convergent finding rather than a circular one.

Beyond these objective metrics, Alexander (2002–2005) proposed the *mirror-of-the-self* test as a perception-based instrument. Faced with two design alternatives, an observer is asked which more closely resembles their own self. Administered pairwise across many observers, the test produces remarkably consistent judgments and provides a phenomenological anchor for the analytical machinery introduced above.

These instruments are partial. Formal definitions of the fifteen properties and of the scores — their dimensional composition and grading — are set out in the cited primary sources (Alexander, 2002–2005; Jiang & de Rijke, 2023; Jiang, 2025). The B-score in particular depends on the prompt and the vision model that reads the image, and may inherit its training-data and cultural biases; its stability across repeated runs and prompts (single-run intraclass correlations near 0.75) and its relation to independent human ratings are documented in those sources (Jiang, 2025; Xue & Jiang, 2026). Used as instruments of structured comparison rather than oracles of objective beauty, they convert architectural intuition into something that can be discussed, taught, and used to constrain AI.

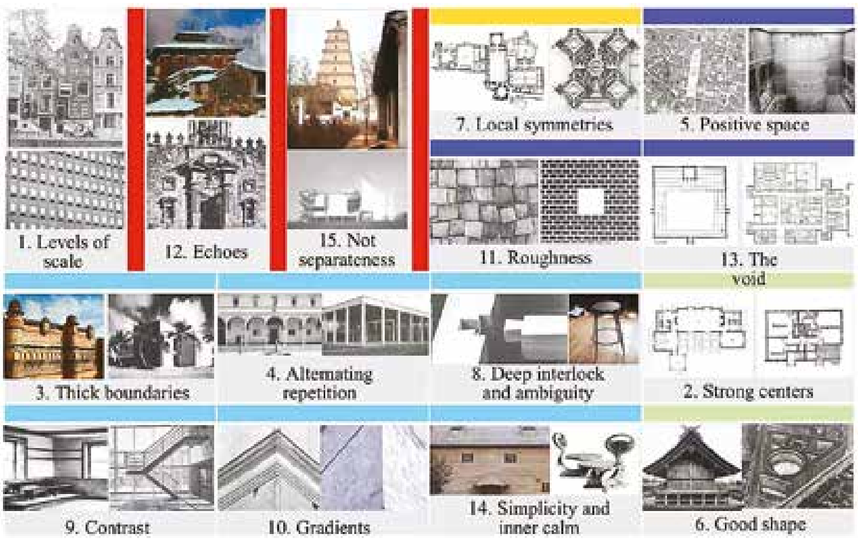

Fig. 2. The fifteen properties of living structure, organised into five groups by importance and scale: three global properties (red) span all scales; local symmetries (orange) form their own group; two blue groups capture local properties at single and at adaptive substructures; strong centres and good shape (green) consolidate the rest. (For interpretation of the references to colour in this figure legend, the reader is referred to the Web version of this article.)

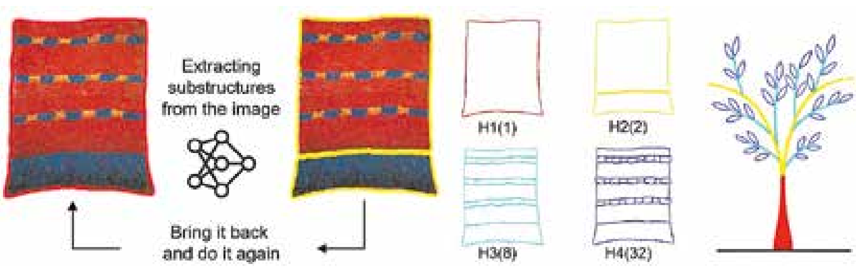

Fig. 3. A carpet pattern recursively decomposed into nested levels H1–H4, with far more small substructures than large ones at each step; the hierarchy yields an L-score of 172. The same recursion appears in natural growth.

3. The Living Structure + AI paradigm

The Living Structure + AI paradigm reframes architectural design as a two-stage process: first the deliberate construction of a *structural skeleton* that satisfies living-structure principles, and then the *AI-assisted generation of stylistic skins* on that skeleton. The skeleton carries coherence, hierarchy, and life; the skin carries cultural specificity. The two together yield designs that are structurally coherent yet stylistically diverse (Fig. 4).

3.1. Skeleton: structural order made explicit

The skeleton is generated by iterative subdivision: from a bounding whole, the designer or algorithm subdivides the form into successively finer substructures, ensuring at each step that far more smalls than larges holds, that the 2–6 ratio is respected across levels, and that the hierarchy is articulated through strong centres and well-defined boundaries (Alexander, 2002–2005; Jiang, 2015). The L- and B-scores monitor progress; the skeleton is declared finished only when its hierarchical richness reaches a target. It is not a style — it commits only to a kind of structural order.

3.2. Skin: AI as structural mediator

Once the skeleton is fixed, the skin is generated by AI under structural constraint: diffusion and multimodal models produce stylistic expressions — materials, ornaments, surface articulations — that respect the declared hierarchy. The same skeleton may be clothed in a contemporary Cantonese, Beaux-Arts, or modernist dialect, the skins compared on cultural, climatic, or programmatic grounds.

AI's role shifts decisively. It is no longer a generator of free-floating novelty but a structural mediator — a translator between universal order and particular cultural expression. Stylistic difference is celebrated; structural mediocrity is not. Living Structure + AI binds generative AI to scientific criteria of structural beauty, transforming the architect's role from form-maker to guardian of living structure, supported by but not replaced by AI.

3.3. AI as judge: diagnosis before generation

Boys Smith and Salingaros (2025) presented three pairs of architectural proposals — for a department store on Oxford Street, a sports stadium in Bath, and a high-speed rail viaduct in Solihull — to multiple large language models. Each pair contrasted a contemporary scheme with a more traditional, human-scaled alternative, prompted with two complementary criteria sets: ten emotional descriptors from neuroaesthetics and Alexander's fifteen geometric properties.

The findings were consistent across criteria, prompts, and models: the LLMs preferred the more traditional, human-scaled designs in all three cases, their emotional and geometric verdicts agreed in twenty of twenty repeated runs, and the AI judgments aligned with independently conducted public opinion polls. This is, by the authors' own account, a pilot of only three pairs without formal controls; its weight lies less in sample size than in the agreement of two independently prompted criteria sets and of AI with public polls. Read that way, the correlational chain — living geometry to positive-valence emotions to public preference — offers

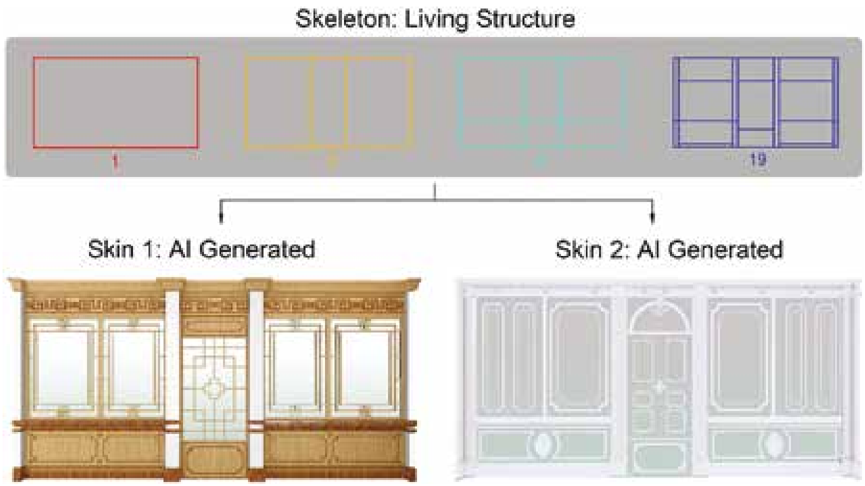

Fig. 4. The skeleton–skin paradigm. A structural skeleton (top) is iteratively subdivided into finer substructures (1 → 3 → 6 → 19) respecting far more smalls than larges and the 2–6 scaling rule; AI then generates stylistic skins (bottom) — contemporary, traditional, regional — on that fixed skeleton.

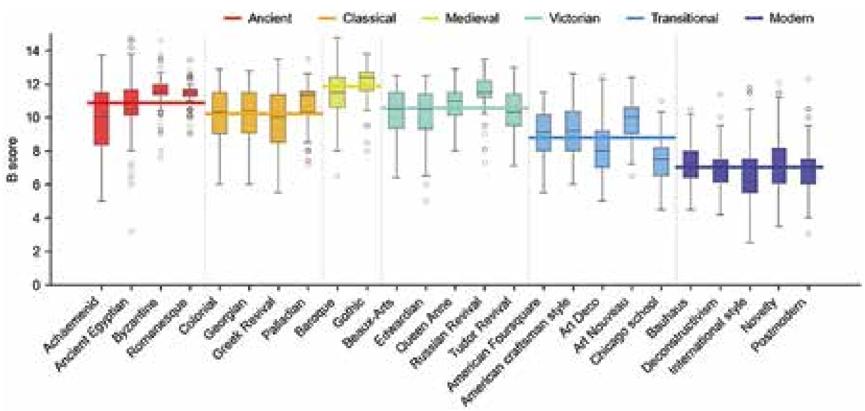

Fig. 5. Distribution of B-scores across 25 western architectural styles, grouped into six historical eras. Pre-industrial styles (Medieval, Classical, Victorian) cluster at higher B-scores; modernist and postmodernist styles cluster at the bottom. The pattern reflects the absence, in modernist forms, of the geometric properties associated with living structure. Adapted from Xue and Jiang (2026).

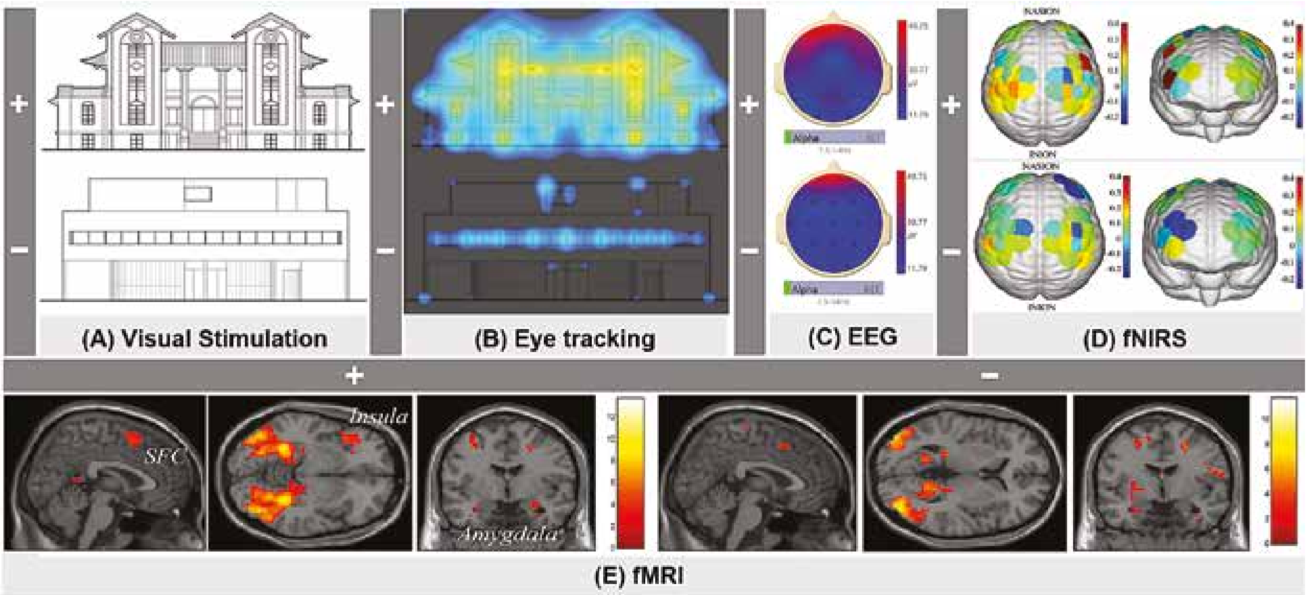

Fig. 6. Multimodal evidence under assembly for the neural reality of structural beauty. The panels show the experimental pipeline — (A) visual stimulation, (B) eye-tracking, (C) EEG, (D) fNIRS, and (E) fMRI. Of these, only the fMRI study is reported and cited in this essay (Yin et al., 2026, in submission); the eye-tracking, EEG, and fNIRS panels illustrate ongoing work and are not used here as evidence.

preliminary support for a long-suspected link between geometric structure and human well-being (Mehaffy & Salingaros, 2015; Salingaros, 2006).

Applied at scale, the same logic exposes a clear pattern across architectural styles. Across 4794 images covering 25 western architectural styles grouped into six historical eras (Xu et al., 2014), pre-industrial styles (Romanesque, Gothic, Byzantine, Medieval, Classical) tend to receive higher B-scores than modernist and postmodernist styles (Fig. 5); in this particular dataset and prompt, medieval examples are preferred over modernist ones in almost all pairwise comparisons (Xue & Jiang, 2026). This contrast should be read with care. Era, building function, image source, and sampling are not controlled, and the result reflects the scored geometric properties rather than a blanket verdict on any style or period. Read narrowly, it suggests that the modernist examples in this sample express fewer of the properties — levels of scale, thick boundaries, alternating repetition, not-separateness — that the B-score rewards; it does not establish that modern materials or ambitions are incompatible with living structure.

A third, still-unpublished line points the same way. Using the Beautimeter to score sixty matched images across geometric patterns, architectural details, and building facades, we conducted an fMRI study with 63 participants (Yin et al., 2026, in submission). High-livingness images were rated more likable, more living, and more complex, with forced-choice preferences rising from 78 percent (patterns) to 85 percent (details) to 88 percent (facades). The most robust neural effect was perceptual: stronger activation for high-livingness images in occipital and ventral temporal visual cortex, surviving whole-brain FWE correction. Valuation-related effects were weaker and conditional — vmPFC decoding emerged only after small-volume correction, and caudate-head activation only as a trait-dependent association with self-inclusion of the built environment. The pattern is consistent with livingness being encoded primarily in perceptual systems; but, as a single not-yet-reviewed study, it is a suggestive bridge between organised multiscale structure and aesthetic experience rather than a settled one (Fig. 6).

These three lines — Beautimeter analysis at scale, the LLM-as-judge pilot, and the fMRI experiment — point in the same direction: that a measurable part of architectural preference tracks structural properties rather than taste alone. The claim is one of central tendency, not consensus. A substantial majority, on the order of four in five viewers, tend to agree on which of two buildings is more living when judged through the fifteen properties; a real minority do not, and aesthetic response remains shaped by culture, memory, and context. Two of the three lines (the LLM-as-judge pilot and the fMRI study) are recent and, respectively, based on a small sample and not yet peer-reviewed. They are offered as convergent but preliminary support — consistent with a forum essay that argues a position from cited work rather than reporting primary data — and the case for objective beauty is correspondingly advanced as a defensible hypothesis, not a closed question.

3.4. From judge to co-designer

The natural next step is to close the loop. AI judgments can be fed back into generation: a first draft is produced, diagnosed for weak properties, then iterated to strengthen them — AI evolving from one-shot stylist to iterative partner in structural refinement. Its most consequential leverage lies not in "zero-to-one" novelty but in taking the existing spaces around us — homes, classrooms, offices, hospitals, streets — that are merely adequate and making them more alive, without demolishing what is there. The paradigm is not a return to historicism nor a rejection of contemporary materials; it simply insists that experimentation occur on a structurally well-formed skeleton. Many skins, including radically modern ones, can satisfy the criteria. The aim is structure *before* style — not structure *instead of* style.

Fig. 7. Classroom W1-233 before and after renovation. Top: original room with undifferentiated long wall. Middle: declared skeleton (six levels of scale, 2–6 ratio). Bottom: realised renovation — paneling, mouldings, framed artworks — expressing the skeleton. L-score rose by an order of magnitude; mirror-of-the-self preference favoured the renovated condition (Table 1).

4. Four renovations on the HKUST(GZ) campus

4.1. Setting and pedagogy

Theory must be tested in real space. Over the last two academic years, LivableCityLAB at HKUST(GZ) has used the Living Structure + AI paradigm as the basis of a series of teaching-led renovations on campus. Four spaces have been studied in detail: Classroom W1-233, Student Activity Centre 5A-220, Office E3-312, and Meeting Room E3-314 — originally typical contemporary interiors, visually flat and low in perceptual vitality, redesigned by students under the skeleton–skin workflow and realised on site by professional contractors. Several cohorts of students, both undergraduates and postgraduates, completed design-–experience–evaluation cycles in which AI tools were used selectively for skin generation, property checks, and rapid feedback, while structural decisions were made by students with supervisor support. The students' role was to measure the rooms, declare the skeleton, evaluate AI-generated skins, follow the build, and inhabit the renovated spaces afterwards — an emphasis on experiential learning that kept L- and B-scores anchored in what the spaces actually felt like.

4.2. Classroom W1-233

The original classroom was a long rectangular room with one undifferentiated white wall, an unarticulated ceiling, and mass-produced furniture. Students mapped the long wall and proposed a skeleton of three bays, then thirteen panels, then 45, 145, 382, and 1314 substructures across six levels — an L-score of about 11,400 with full compliance to the 2–6 scaling rule (Jiang et al., 2026).

The finest subdivision was simplified for construction. The

Table 1 Summary of the four HKUST(GZ) campus case studies: declared skeleton, evaluation instruments, and the direction of change after renovation. Evidence is convergent and directional rather than inferential; human preference was assessed by pairwise mirror-of-the-self comparison with student cohorts (not blinded, randomised, or preregistered), and L-/B-scores and 3M VAS maps were computed before and after. Arrows denote increase. Full per-case values, image sets, and immersive renderings are accessible in the Data Availability; consistent with a forum essay, this paper summarises rather than reproduces those data.

Case	Declared skeleton	Evaluation instruments	Change after renovation
Classroom W1-233	6 levels; declared L ≈ 11,400 (simplified for build)	L-score; B-score; mirror-of-the-self (pairwise)	↑ L, ↑ B; renovated condition preferred by most students
Activity Centre 5A-220	Nested centres across multiple levels	L-score; B-score; mirror-of-the-self; 3M VAS	↑ L, ↑ B; renovated preferred; VAS attention consolidates into focal centres
Office E3-312	6 levels of scale	L-score; B-score; mirror-of-the-self; 3M VAS	↑ L, ↑ B; renovated preferred; VAS attention concentrates on dense hierarchy
Meeting Room E3-314	Multiple levels; modest, reversible	L-score; B-score; mirror-of-the-self (pairwise)	↑ L, ↑ B; renovated condition preferred in pairwise tests

realised renovation introduced paneling, mouldings, framed artworks, and articulated boundaries on the long wall, with subtle articulation of the ceiling and entrance. Fig. 7 shows a classroom of the same size, furniture, and programme. In pairwise mirror-of-the-self comparisons the renovated condition was preferred by most participating students, and both L- and B-scores rose; the four cases, their instruments, and the scope and limits of their evaluation are summarised in Table 1, with full per-case records reported in the Data Availability section at the end of the paper (Jiang, 2025)

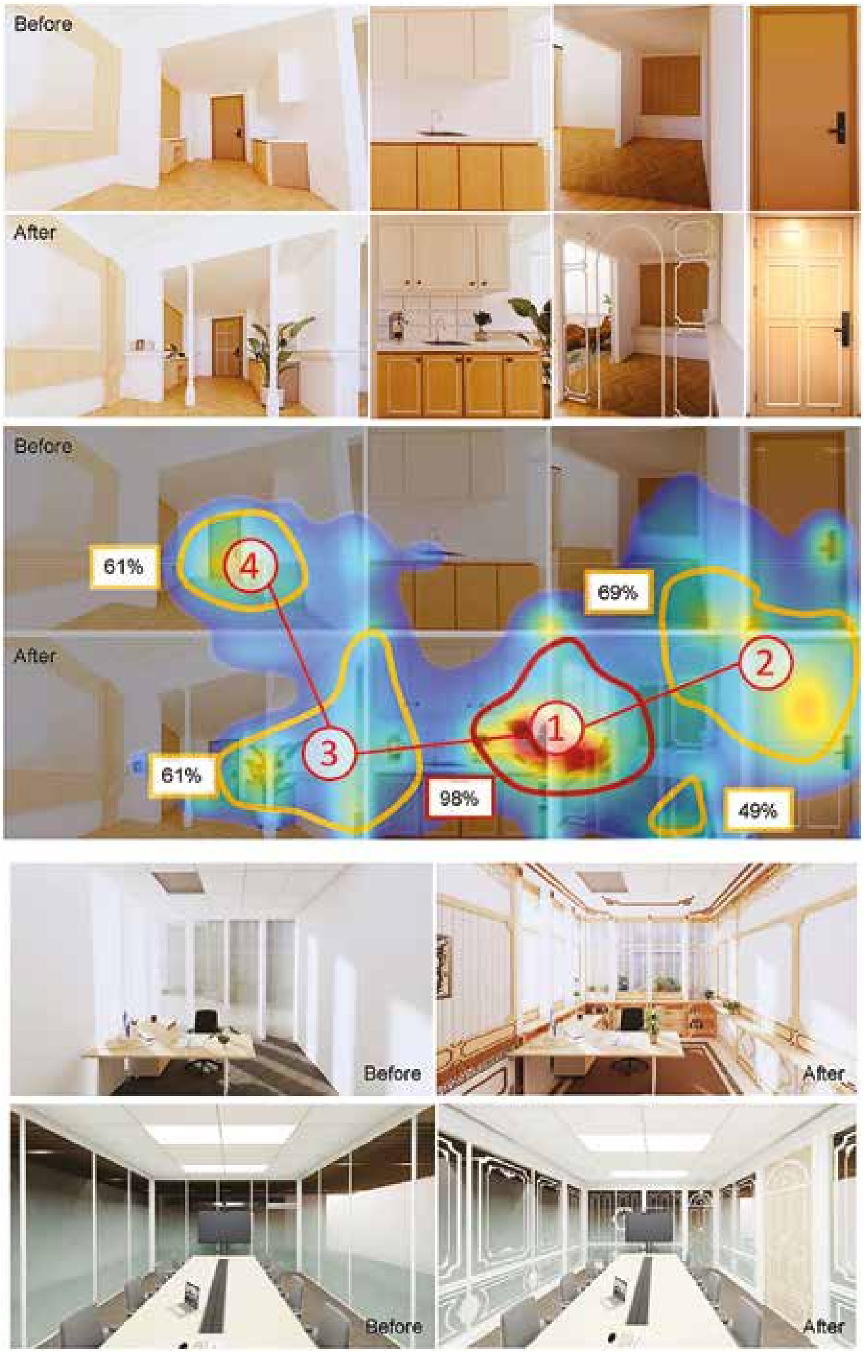

Fig. 8. Three campus renovations — Activity Centre 5A-220, Office E3-312, and Meeting Room E3-314 — each showing the original interior, the declared skeleton, and the realised result. Across all three, L- and B-scores rise and mirror-of-the-self preference shifts toward the renovated condition (Table 1).

4.3. Student Activity Centre 5A-220

The activity centre is a multifunctional space combining a lounge, entry foyer, and wall-rest zone. The original space was visually flat — walls undifferentiated, transitions unmarked. Students worked in small teams under a common skeletal logic, introducing nested centres, articulated boundaries, and fine-grained substructures while preserving the openness and adaptability of the functional programme.

Here the team also applied 3M Visual Attention Software (Salingaros & Sussman, 2020): the pre-renovation heatmap showed diffuse attention, the post-renovation one clear focal centres and continuous paths at multiple scales (Table 1) — visual attention thus tracking the L- and B-score gains.

4.4. Office E3-312 and meeting room E3-314

The office and meeting room cases extend the workflow into work-oriented settings (Fig. 8): the same skeleton–skin logic, applied through modest, reversible, inexpensive means — paneling, framing, mouldings, lighting — with the changes summarised in Table 1 and immersive renderings of all four cases online at the Data Availability.

4.5. What the cases show

Three lessons stand out. First, the skeleton–skin workflow is teachable to students without architectural backgrounds — robust enough to communicate quickly, rigorous enough to discipline AI-generated skins. Second, the renovations are governance-friendly: incremental, reversible, low-carbon, respectful of existing footprints. Third, across methodologically distinct instruments (Table 1), structural metrics and perceptual judgments move together — convergent, directional evidence rather than a controlled trial.

5. From buildings to cities: implications for science, education, and governance

5.1. Urban informatics from description to design

Whether the paradigm scales beyond single rooms is, at this stage, a hypothesis rather than a demonstrated result: the campus cases concern interiors, and the move to urban fabric, renewal, education, and policy that follows should be read as an agenda for research rather than a claim already evidenced. With that caveat, the Living Structure + AI paradigm extends from the classroom toward the city, joining an emerging programme on urban informatics in the service of livable cities (Jiang et al., 2026). Urban informatics describes cities in extraordinary detail (Batty, 2013) and predicts where congestion will form or heat islands emerge (Zhang et al., 2018). What it has done less well is articulate what cities *ought* to be. The science of living structure offers one route from "is" to "ought": if we can measure how alive an environment is, we can aim for environments that score higher, connecting structural quality to health, well-being, and place attachment (Jiang, 2025; Jiang & de Rijke, 2023).

5.2. The universal structural backbone

A central finding of structure-based urban science is the near-universality of the scaling law: from medieval European towns to historic Chinese cities, the same pattern recurs — far more small structures than large, in nested hierarchies (Jiang & Yin 2014; Jiang, 2015). Modernist plans often invert or flatten this hierarchy, with consequences others have linked to disorientation and social dysfunction (Curl, 2018; Jacobs, 1961). The scaling law offers a computable test of whether an urban form is structurally well-formed, independent of style.

AI enters urban informatics in the same way it enters architecture. Diagnostically, vision–language models can score street segments, neighbourhoods, and public spaces against living-structure criteria. Generatively, AI can propose skeleton-respecting interventions that increase hierarchical richness without demolishing existing fabric. The paradigm underwrites urban renewal as careful, additive, and structurally guided rather than as wholesale replacement (Mehaffy & Salingaros, 2015; Jiang, 2025).

5.3. Structural beauty across urban scenes

Structural beauty is also distributed unevenly across the city. Applied at scale to typed urban scenes (Jiang, 2025), B-scores cluster by category: industrial scenes lowest, then business, a broad band of living scenes, public scenes higher, and cultural scenes (castles, churches, palaces) highest (Fig. 9). The ordering tracks how far each category supports the geometric properties of living structure —deeper hierarchies, more alternating repetition, stronger centres — complementing the style-based analysis of Fig. 5.

Read alongside the LLM-as-judge and fMRI results, the distribution suggests — though it does not prove — that the felt quality of a city is partly the product of the buildings composing it, scored on living-structure criteria. On this reading, renewal strategies could be assessed in part by their effect on the distribution in Fig. 9.

5.4. Education, practice, governance

The paradigm has direct implications across three fronts. For *education,* curricula should be organised around reading built environments structurally, declaring and verifying skeletons before generating skins, and using AI as a structural mediator in dialogue with L- and B-scores — neither anti-AI nor uncritically pro-AI, but structure-first.

For *practice,* since most of the spaces that need to become more alive already exist, Living Structure + AI proposes a third path between leaving buildings untouched and demolishing them: incremental, reversible structural enrichment through skeleton-respecting interventions — faster, cheaper, lower-carbon, and more respectful of communities than demolition-driven redevelopment (Mehaffy & Salingaros, 2015; Jiang 2025).

For *governance,* pre-occupancy AI evaluation can flag designs that fail living-structure criteria (Boys Smith & Salingaros, 2025), and L-scores, B-scores, and mirror-

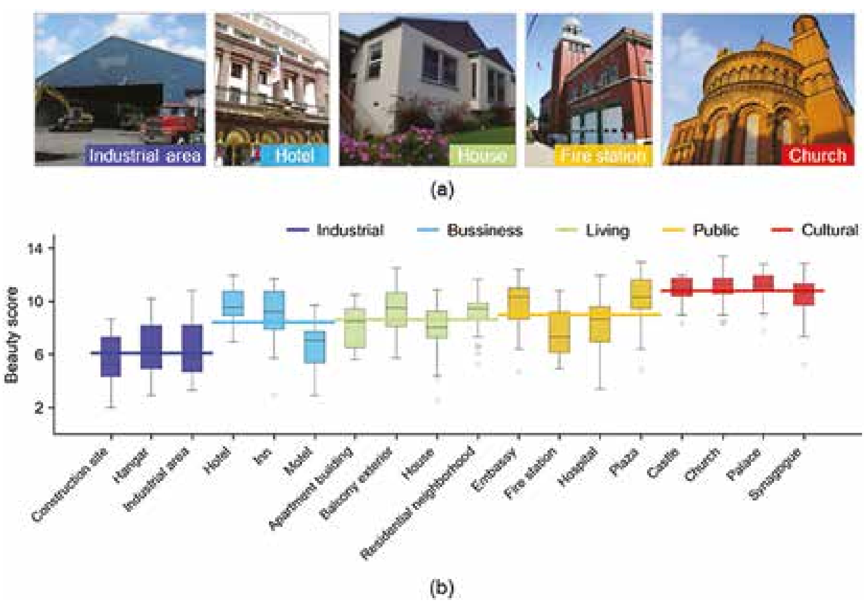

Fig. 9. B-scores across nineteen classes of urban scenes, regrouped into five categories. Cultural scenes (castles, churches, palaces) cluster at the top, industrial scenes at the bottom, reflecting how far each supports the properties of living structure. Adapted from Xue and Jiang (2026).

of-the-self surveys could in principle give municipalities a supplementary, quantitative input into renewal decisions.

Whether such metrics can be embedded in actual planning, legal, and participatory processes is an open institutional question well beyond the evidence assembled here; the path from interior cases and image scoring to municipal practice is offered as a research agenda, not a demonstrated result — a hoped-for shift from *cold technology toward warm intelligence* in which warmth, coherence, and felt life become primary objectives rather than residual outputs.

6. Conclusion: A quieter and better future for AI in architecture

Generative AI entered architecture loudly. This essay has argued that its most valuable contribution lies elsewhere: not in spectacle but in the quiet work of structural diagnosis and structurally constrained generation. The Living Structure + AI paradigm offers one concrete way to organise that contribution — distinguish skeleton from skin, declare and verify the skeleton before AI generates the skin, and anchor evaluation in structural metrics and embodied perceptual tests. The four HKUST(GZ) renovations show that structurally informed, AI-supported interventions produce measurably more coherent environments without large budgets, demolition, or stylistic ideology.

Three lines of work seem especially promising: subdivision algorithms that generate skeletons from boundary conditions; AI judges that build on the Beautimeter and LLM-as-judge experiments; and policy adoption that incorporates structural metrics into approval, procurement, and education. AI is not the cause of architecture's recent troubles, nor their cure; but embedded in a paradigm that takes structure seriously, it can become an instrument for making more places, in more cultures, more alive. Beauty, as Christopher Alexander wrote, is not about how something looks but about how it is — and this paradigm is, in the end, an argument for taking that sentence seriously.

Data availability

The four interactive case studies are accessible at the following links:

- Classroom W1-233: https://vr.justeasy.cn/view/174v3j47i0470778-1734793858.html
- Student Activity Center 5A-220: https://vr.justeasy.cn/view/147e374o54n19057-1753083138.html
- Office E3-312: https://vr.justeasy.cn/view/zn61187413306813-1756382846.html
- Meeting Room E3-314: https://vr.justeasy.cn/view/uk17d1411920b639-1758796620.html

Funding sources

This research is funded by AI Research and Learning Base of Urban Culture under Project 2023WZJD008, Guangdong Provincial Key Lab of Integrated Communication, Sensing and Internet of Things grant number [2023B1212010007].

The Hong Kong University of Science and Technology (Guangzhou) grant number [G0101000142], the City-University Joint Fund of the Science and Technology Project of Guangzhou grant number [2024A03J0529]

Declaration of competing interest

The author declares that they have no known competing financial interests or personal relationships that could have appeared to influence the work reported in this paper.

Acknowledgements

This paper was prepared with the assistance of Claude 4.7, but the author takes full responsibility for any errors or oversights. I thank my students and colleagues, both current and former, at LivableCityLAB and the Urban Governance and Design Thrust at HKUST (GZ). I am grateful to Nikos A. Salingaros and Nicholas Boys Smith for the work on AI as a judge of architecture, and for many illu- minating conversations on living geometry and human-centered design.

References

Alexander, C. (1979). *The timeless way of building*. New York: Oxford University Press.

Alexander, C. (2002). *The nature of order: An essay on the art of building and the nature of the universe, volumes 1–4, center for environmental structure.* Berkeley.

Alexander, C., Ishikawa, S., & Silverstein, M. (1977). *A pattern language: Towns, buildings, construction.* New York: Oxford University Press.

Architecture Education Declares. (2019). *Open letter on architectural education*. https://livablecitylab.hkust-gz.edu.cn/ArchitectureEducationDeclares/.

Bak, P. (1996). *How nature works: The science of self-organized criticality.* New York: Springer.

Batty, M. (2013). *The new science of cities.* Cambridge, MA: MIT Press.

Boys Smith, N. (2016). *Heart in the right street: Beauty, happiness and health in designing the modern city, London: Create Streets.*

Boys Smith, N., & Salingaros, N. A. (2025). AI judging architecture for well-being: Large language models simulate human empathy and predict public preference. *Designs, 9*(5), 118.

Curl, J. S. (2018). Making dystopia: The strange rise and survival of architectural barbarism. In M.

del Campo, & N. Leach (2022), *Machine hallucinations: Architecture and Artificial intelligence (special issue), Architectural design, 92*. London: Oxford University Press.

Eglash, R. (1999). African fractals: *Modern computing and Indigenous design*. New Brunswick: Rutgers University Press.

Gehl, J. (2010). *Cities for people*. London: Island Press.

Heatherwick, T. (2023). *Humanise: A maker's guide to designing our cities*. London: Penguin.

Jacobs, J. (1961). *The death and life of great American cities*. New York: Random House.

Jiang, B. (2015). Geospatial analysis requires a different way of thinking: The problem of spatial heterogeneity. *GeoJournal, 80*(1), 1–13.

Jiang, B. (2019). Living structure down to earth and up to heaven: Christopher Alexander. *Urban Science, 3*(3), 96.

Jiang, B. (2025). Beautimeter: Harnessing GPT for assessing architectural and urban beauty based on the 15 properties of living structure. *AI, 6*(4), 74.

Jiang, B., Yao, Q., Qian, H., & Hu, B. (2026). Towards the science of living structure: Making and remaking livable cities as part of urban informatics. *Urban Informatics, 5*, 15.

Jiang, B., & de Rijke, C. (2023). Living images: A recursive approach to computing the structural beauty of images or the livingness of space. *Annals of the Association of American Geographers, 113*(6), 1329–1347.

Leach, N. (2023). *Architecture in the age of artificial intelligence*. London: Bloomsbury.

LivableCityLAB. (2025). *Living structure: Exploring the beauty of Chinese traditional buildings through the lens of AI*. Beijing: China Architecture and Building Press (in Chinese).

Mandelbrot, B. B. (1982). *The fractal geometry of nature*. New York: W. H. Freeman.

Mehaffy, M. W. (2020). *Cities alive: Jane Jacobs, Christopher Alexander, and the roots of the new urban Renaissance*. Portland: Sustasis Press.

Mehaffy, M. W., & Salingaros, N. A. (2015). *Design for a living planet: Settlement, science, and the human future*. Portland: Sustasis Press.

Salingaros, N. A. (2006). *'A theory of architecture. Solingen: Umbau-Verlag*.

Salingaros, N. A., & Sussman, A. (2020). Biometric pilot studies reveal the arrangement and shape of windows on a traditional facade to be implicitly engaging, whereas contemporary facades are not. *Urban Science, 4*(2), 26.

Tobler, W. (1970). A computer movie simulating urban growth in the Detroit region. *Economic Geography, 46*, 234–240.

Xinhua News Agency. (2025). The central urban work conference was held in Beijing, and Xi Jinping delivered an important speech. https://www.gov.cn/yaowen/liebiao/202507/content_7032083.htm.

Xu, Z., Tao, D., Zhang, Y., Wu, J., & Tsoi, A. C. (2014). Architectural style classification using multinomial latent logistic regression. In *Computer vision – ECCV 2014* (pp. 600–615). Springer.

Xue, J., & Jiang, B. (2026). *Computing and interpreting structural beauty across architectural styles and urban scenes*. Working paper, HKUST(GZ).

Yin, J., Yin, L., Du, J., Yang, D., Hu, B., & Jiang, B. (2026). *Neural correlates of architectural livingness: An fMRI study with structural prompting* (In submission).

Zhang, F., Zhou, B., Liu, L., et al. (2018). Measuring human perceptions of a large-scale urban region using machine learning. *Landscape and Urban Planning, 180*, 148–160.

AGR integrates Septentrio GNSS for resilient UAV navigation

Combined with AGR's proprietary integrated navigation strategies and flight control system (AG6), this creates an industrial UAV platform capable of maintaining precise, stable, and safe navigation in demanding environments. The mosaic-G5 P3 supports multi-frequency, multi-constellation GNSS reception with low and predictable latency needed for stable and accurate control systems. It leverages AIM+ Advanced anti-jamming and spoofing detection technology for reliable flights in interference-risky zones. Building on this, AGR employs integrated navigation strategies (GNSS/IMU fusion), visual-aided navigation, robust anomaly detection mechanisms, and high-performance flight control algorithms. *www.septentrio.com*

UAVOS introduces NAVAI vision

UAVOS has successfully tested NAVAI, a vision-based navigation module for unmanned aircraft systems designed to improve flight resilience when GNSS signals are degraded or temporarily unavailable. It uses neural networks to match real-time camera imagery with pre-loaded terrain maps, helping unmanned aircraft estimate their position by matching real-time camera imagery with pre-loaded terrain maps. *www.uavos.com*

Emesent secures $17million

Emesent, Australia, has secured $17m in new funding to accelerate development of its Cortex AI autonomy platform and expand its Aura cloud software offering. It comprises a $7m venture debt facility from Australia's NRFC and a $10m equity round by Main Sequence, QIC Ventures, Orion Resource Partners, Hostplus and NGS Super. *www.emesent.com*

Trimble PX-1 RTX powers BVLOS drone delivery

Volatus Aerospace Inc. Canada, has integrated the Trimble PX-1 RTX solution into its commercial drone fleet to enhance positioning accuracy, operational reliability and flight safety. It uses drones to conduct routine deliveries of medical supplies in Alberta. The company selected the Trimble PX-1 RTX system to provide cm-level positioning and precise heading information for its Canary delivery drone platform, enabling accurate navigation during fully remote operations.

GNSS (SBAS) Constellation Specific Monthly Analysis Summary: June 2026

The analysis performed in this report is solely the author's work and his opinion.

Narayan Dhital
Actively involved to support international collaboration in GNSS-related activities. He has regularly supported and contributed to different workshops of the International Committee on GNSS (ICG), and the United Nations Office for Outer Space Affairs (UNOOSA). As a professional employee, the author is working as GNSS expert at the Galileo Control Center, DLR GfR mbH, Germany.

Introduction

This article continues the monthly performance analysis of the GNSS/SBAS constellation. Readers are encouraged to refer to previous issues for foundational discussions and earlier results. The focus for this month's issue is a preliminary assessment of Dual Frequency Multi Constellation (DFMC) SBAS. The goal is to examine representative DFMC SBAS test-bed data and compare the DFMC integrity concept with legacy single-frequency SBAS. Particular attention is given to DFC corrections, DFRE residuals, sigma construction and protection level generation.

1. Introduction

Legacy SBAS relies on a single-frequency measurement and therefore requires ionospheric corrections and GIVE bounds. The user variance model is largely driven by UDRE and GIVE parameters. In DFMC SBAS, dual-frequency ionosphere-free measurements remove the dominant first-order ionospheric effect. Consequently, DFMC introduces Dual Frequency Corrections (DFC), DFRE monitoring, degradation models and revised variance propagation. The integrity budget shifts from prominent ionospheric uncertainty to correction, residual uncertainty and geometry. Details on the technical terms (like UDRE, GIVE..) and mathematical parts can be found in this analysis published in mycoordinates: https://mycoordinates.org/gagan-performance-assessment-for-aircraft-precision-approach/.

Similarly, for the DFMC technical terms and mathematical parts, readers are encouraged to read this article: https://curate.curtin.edu.au/articles/journal_contribution/Preliminary_Performance_Analysis_of_a_Prototype_DFMC_SBAS_Service_over_Australia_and_Asia-Pacific/31708315?file=62761321

Message Structure Differences

In L1 SBAS, integrity is driven by UDRE and GIVE concepts. In DFMC SBAS, the system broadcasts DFMC-specific correction and integrity information. The central user concepts become DFC, DFC Sigma, DFRE and degradation terms. The user no longer depends on a sampled ionospheric grid for routine positioning.

DFMC SBAS differs fundamentally from legacy single-frequency SBAS because the user no longer relies on SBAS ionospheric grid corrections and GIVE integrity bounds. Instead, dual-frequency measurements (e.g., GPS L1/L5 or Galileo E1/E5a) form an ionosphere-free observable that removes the dominant first-order ionospheric error directly. As a result, the traditional fast correction, long-term correction and ionospheric correction framework of L1 SBAS is replaced by a correction-residual framework based on Dual-Frequency Corrections (DFC), DFC sigma, DFRE sigma and degradation terms. While the underlying satellite clock and orbit corrections still exist within the ground segment, they are effectively merged into the DFC information supplied to the user, greatly simplifying user processing. The elimination of ionospheric grid messages also makes DFMC SBAS significantly more efficient in terms of GEO broadcast bandwidth, allowing that capacity to be used for multi-constellation support and enhanced integrity information. The integrity focus therefore moves toward correction residual bounding represented by DFC and DFRE uncertainties.

Dataset

The dataset analyzed corresponds to SouthPAN DFMC SBAS test-bed observations processed with gLAB using GPS and Galileo. The selected date is day of year 183, 2019. Statistics and plots are generated from DFMC correction, variance and SBAS output files. The data is taken from this server: https://server.gage.upc.edu/PhD/Ibanez_Deimos/Ibanez_Deimos_Phd_files.7z.

2. Results and Interpretation

Figure 1 shows HPL95 of 13.11 m

and VPL95 of 20.55 m. Both remain comfortably below LPV-200 alert limits of 40 m and 35 m. Protection-level peaks coincide with reductions in the number of satellites used. This demonstrates that geometry remains a dominant driver of integrity performance even in DFMC SBAS. The large spike around 16.5 hours appears to be associated with a temporary degradation in geometry and/or integrity bounding rather than a persistent increase in ranging uncertainty.

In Figure 2, GPS and Galileo exhibit nearly identical behaviour. Mean total sigma is approximately 1.23 m for both constellations and the 95th percentile remains near 1.55–1.57 m. The similarity indicates consistent treatment of both constellations inside the SouthPAN DFMC processing chain. The recurring U-shaped trajectories correspond to elevation-dependent error behaviour, where multipath, receiver noise and atmospheric mapping effects increase at lower elevations.

Figure 3 provides the strongest evidence of the DFMC integrity philosophy. DFC sigma is the largest contributor throughout most of the day. Receiver and multipath terms are secondary contributors. Tropospheric uncertainty

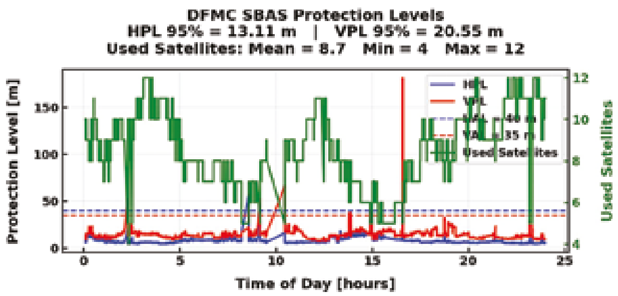

Figure 1: HPL, VPL and number of satellites used.

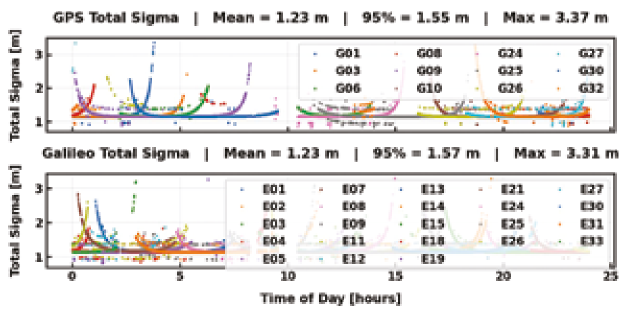

Figure 2: GPS and Galileo total sigma distributions.

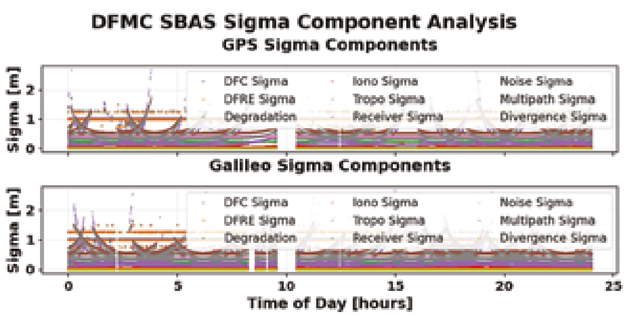

Figure 3: Sigma component decomposition.

remains modest. The ionospheric sigma contribution is nearly negligible compared with DFC and receiver-related terms. This is a fundamental departure from single-frequency SBAS where ionosphere frequently dominates the protection-level budget. The resemblance between GPS and Galileo component distributions further indicates a harmonized DFMC integrity model.

3. Conclusion

Overall, Figure 3 shows that DFC sigma is the dominant contributor to the integrity budget, while ionospheric sigma is almost negligible; Figure 2 shows that GPS and Galileo maintain nearly identical total sigma performance, with 95th-percentile values around 1.55–1.57 m; and Figure 1 shows that despite a few geometry-driven events, HPL95 and VPL95 remain well below LPV-200 alert limits. Together, the three figures illustrate the central objective of DFMC SBAS: integrity performance is no longer limited by ionospheric uncertainty but is instead governed primarily by correction residuals, receiver effects and satellite geometry.

In DFMC SBAS, ionospheric uncertainty is largely removed by the dual-frequency observable. The limiting factor therefore becomes confidence in the broadcast correction itself and the residual error remaining after monitoring. DFC sigma and DFRE sigma provide conservative bounds on those residuals. The results reveal that correction uncertainty—not ionosphere—is now the principal contributor to the integrity budget. This behavior is exactly what would be expected from a mature DFMC SBAS architecture.

The analyzed representative SouthPAN test-bed dataset demonstrates successful DFMC SBAS performance. Protection levels remain well below alert limits, GPS and Galileo show nearly identical statistics, and the sigma budget confirms the migration from ionosphere-driven integrity to correction-driven integrity. The plots collectively demonstrate how DFC residual uncertainty, receiver effects and geometry govern user protection levels in modern DFMC SBAS systems.

Data sources and Tools:

https://cddis.nasa.gov (Daily BRDC, RINEX OBS); http://ftp.aiub.unibe.ch/CODE_MGEX/CODE/ (Precise Products); BKG "SSRC00BKG" stream; IERS C04 ERP files

SBAS Mentor, ESA

gLAB GNSS, https://gage.upc.edu/en/learning-materials/software-tools/glab-tool-suite

serenad-public.cnes.fr (SBAS data)

AITL-WING-HITL: Telemanipulation of autonomous drones using DTs of aerial traffic interfaced with WING

The system is designed to intervene in scenarios, where an autonomous AI agent – the "new driver" – encounters conditions too complex or unorthodox for autonomy alone to handle. We present here the concluding part of the paper. The first part was publsihed in June'26 issue

Kaya Kuru
School of Engineering and Computing, University of Central Lancashire, Preston, PR1 2HE, UK
Software Engineering Department, Fenerbahce University, Ataşehir, İstanbul, 34758, Turkey

Benjamin J. Watkinson
School of Engineering and Computing, University of Central Lancashire, Preston, PR1 2HE, UK

Claire Tinker-Mill
School of Engineering and Computing, University of Central Lancashire, Preston, PR1 2HE, UK

Sam Worthington
Worthington Sharpe Ltd., Unit 1.3s Halton Mill, Mill Ln, Halton, Lancaster LA26ND, UK

Keith Vinning
PilotAware Ltd., 19 John McGuire Crescent, Coventry, CV32Q, UK

Darren Ansell
School of Engineering and Computing, University of Central Lancashire, Preston, PR1 2HE, UK

Lee Moore
PilotAware Ltd., 19 John McGuire Crescent, Coventry, CV32Q, UK

John M. Pinder
School of Engineering and Computing, University of Central Lancashire, Preston, PR1 2HE, UK

Chris Gilbert
PilotAware Ltd., 19 John McGuire Crescent, Coventry, CV32Q, UK

Aadithya Sujit
School of Engineering and Computing, University of Central Lancashire, Preston, PR1 2HE, UK

David Jones
School of Engineering and Computing, University of Central Lancashire, Preston, PR1 2HE, UK

4. Experimental design

The developed platform – AITL-WING-HITL – needs to be assessed first in the environment of a simulation, then in the drone containment cage, and finally in real-field environments to ensure that the targeted objectives are achieved. The performance of humans while teleoperating multiple A-UAVs using the WING, as well as the functions of the platform, was evaluated in the simulation module of the developed platform. Volunteers were needed to test the developed platform for an hour, which aims to investigate further advancements through scenario-based experiments to improve the techniques and approaches before real-world tests. The AITL-WING-HITL platform, with simulation capabilities (Supplement III (Fig. 2, G.1)), provides an easy way to establish varying scenarios with multiple A-UAVs with their particular routes. One HTM can manipulate multiple drones using one WING in a one-to-many intervention mode. We would like to measure if the HTM can adjust their hand impedance sufficiently —

application of hand force and releasing of the force (i.e. the translated input force into sub-movement microstructure states in Supplement I: Yaw (Tables I, II, Figs. 1, 2) and Roll (Tables III, IV, Figs. 3, 4) and Pitch (Tables V, VII, Figs. 5, 6) channels) at the desired time intervals to trigger the targeted actuation. Several scenarios were generated to measure (i) the capability of the user in adapting to the dynamically scaling DT environments and (ii) the efficiency of the responses to different scenarios using the WING with the various intervention modes (Fig. 15). HTMs are expected to improve their skills in real-world implementations as they immerse themselves in the platform over time, using the relation between the amplitude of the mouse movement, which is based on the force applied in channels, and the observed actuation displayed on the interface.

4.1. Policies followed before, during and after the experiment

Participation in the experiments was entirely voluntary, and participants were free to withdraw from the study at any time without providing a reason. No personally identifiable information was recorded, and all data were fully anonymised. Participants granted permission for the experimenter to access anonymised system-generated data and anonymised questionnaires completed during the study. Individuals with diagnosed chronic conditions (e.g. epilepsy) were not permitted to participate. Participants were informed that the anonymised data would be used for research purposes and shared with the academic community through publications. All data will be securely stored and protected for the next seven years in accordance with ethical guidelines (Section 10).

4.2. Environmental settings

University staff and students were voluntarily registered for the evaluation of the AITL-WING-HITL platform through some designed scenarios. An individual's designated code, age and sex information were recorded; no other personal information was registered. The demographics of participants are shown in Supplement-V (the third column of Table 1). The age ranges from 19 to 55. No volunteer came forward from the female gender group, where the number of females is significantly less than the number of males gender in the School of Engineering and Computing from which most of the participants volunteered. The participants are grouped into sub-classes as experienced staff, non-experienced staff, experienced students and non-experienced students as displayed in Supplement-V (the second column of Table 1) based on the second and third questions in the Overall Quality Questionnaire (OQQ) (Supplement IV Table 2). The participants who both answered the second question as "e" (>20) and the third question as "c" (<5 years) or "d" (<10 years) or "e" (>10 years) were grouped as experienced. 4 staff out of 11 and 7 students out of 12 were tagged as experienced (Supplement-V (Table 1)). These sub-groups were incorporated into the analysis of the platform, in particular, the evaluation of the WING's capacity to manipulate A-UAVs, which concerns other close-range aerial vehicles, for the purpose of mitigating collision risks. It is noteworthy to emphasise that discomfort could arise during the non-stop, long test of 6 experimental episodes, and one objective was to measure the emerging discomfort. All participants knew that they could quit the test at any time they wished. Alternatively, the test can be ended by the mentor at any time. In this respect, 3 participants decided to withdraw from the experiment in the middle of the experiment, and the mentor decided to stop the experiment for one of the volunteers due to increasing tension. These volunteers were excluded from the experiment, and no data from these volunteers were included in the assessment of this report. The user-friendly application provides a co-simulation environment coupling real and simulated A-UAVs. Manipulating co-simulated A-UAVs is carried out using the aerial DT interface that is integrated with the WING to avoid the risk of collisions by allowing the user to readily respond to developing situations regarding all other manned or unmanned flights in the environment. The simulation interface makes it easier to repeat the same experiments.

The experimental episodes conducted in this simulated environment were designed to: (i) analyse participants' task performance; (ii) enhance immersive navigation experiences using the WING system to accelerate task performance through human sensorimotor adaptation –where human perception continuously recalibrates in response to new inputs; and (iii) assess Simulation and Cyber Sickness (SCS) symptoms prior to real-world field tests, in order to identify mitigation strategies that improve the functionality of the AITL-WING-HITL platform. Participants were required to complete the Simulation Sickness Questionnaire (SSQ) at three stages: before the orientation training, after the orientation (but prior to the experimental episodes), and after completing all episodes. This allowed for tracking changes in physiological symptoms throughout the experiment. Additionally, they were asked to complete an Overall Quality Assessment Questionnaire (OQQ) at the end of the experiment to evaluate potential areas for further improvement. To maintain experimental continuity and minimise duration, SSQ measurements were not taken between scenarios/ episodes, thereby avoiding interruptions and allowing for an uninterrupted assessment of symptom severity.

A 13-minute orientation was provided to help participants familiarise themselves with the AITL-WING-HITL platform and the WING system. Specifically, the experimental session began with a training phase. Participants first received a brief 5-minute tutorial on the interface, during which the experiment mentor demonstrated how the WING's combined functionalities could be used to control drones via the platform. Key scenarios were demonstrated to clarify the experiment's objectives – for example: "What happens if neither the human nor the system intervenes, resulting in a collision?'' and ''How does the platform autonomously respond to impending, probable, and imminent collision risks using a minimum deviation strategy?'' Following the tutorial, participants engaged in a 7-minute practice session, supported by the experimenter. During this time, they freely explored the system's features to assess how quickly they could adapt to its functionalities. The participants were made aware that the primary objective of the experiment was to avoid collisions using the fewest possible manoeuvres and to maintain minimal deviation from the original flight paths – ensuring safe separation between drones through the WING system.

Each participant was scheduled for an episode duration of seven minutes, with the trial comprising six episodes, each designed to achieve a distinct objective. These episodes incorporated three different scenarios, with each scenario being repeated twice across the six episodes. Based on prior research, it is expected that prolonged continuous exposure can result in more severe symptoms of Simulation Sickness (SS) compared to multiple shorter exposures [46]. Specifically, as observed by Kennedy et al. [47], two key temporal phenomena are associated with SS: the severity of symptoms tends to increase with longer exposure durations during a single session, while repeated exposure to simulation over time can lead to adaptation, reducing symptom severity [46]. To explore these dynamics, the experiment was designed as a continuous, long trial with no breaks between episodes, which may heighten participants' susceptibility to SS if symptoms occur. Each participant completed the full trial in approximately 55 min – comprising a 13-minute orientation followed by six episodes of seven minutes each (6 × 7 = 42 min). If a participant failed an episode (e.g. by causing a collision), the episode was repeated, extending the total trial duration by an additional seven minutes. Although environmental settings remained constant across episode repetitions, participants were instructed to avoid collision risks using different features of the WING system, each involving distinct intervention modes (Fig. 15). Participants could control multiple drones at risk of collision, with capabilities such as altering and locking navigational direction, forcing drones to hover in a safe location, or instructing them to orbit a defined geospatial point until released. All drone movements and granular actuation data were tracked and recorded for later analysis, allowing assessment of both precision and consistency across trials. Participants received real-time warnings upon detection of imminent collision risks. In such cases, the system automatically transitioned from the HOTL state to the HITL state to enable immediate human intervention.

The experiment designed in this study aims to assess both participants' task performance and the unpleasant symptoms experienced during the sessions. Researchers and developers utilising flight simulators or DT technologies must remain mindful of SCS, as it can negatively affect experimental outcomes. Consequently, before widespread adoption, all VR technologies should be rigorously tested for their potential to induce discomfort in users [46]. Analysing the symptoms associated with SCS in relation to specific user interactions within the application can inform system enhancements that may significantly reduce symptom severity. To establish a baseline, participants were assessed prior to the experiment to capture any pre-existing symptoms. This is critical, as individuals can exhibit considerable variability in their tolerance to environmental changes, necessitating pre- and post-test comparisons to determine statistically significant differences. Additionally, a questionnaire (i.e. OQQ), consisting of both Likert-scale and open-ended questions, was administered to evaluate the current functionality of the system and to identify areas for further improvement regarding user experience and task performance. The full questionnaire is provided in the supplementary materials (Supplement IV, Table 2). To measure the severity of SS symptoms, the widely adopted SSQ developed by Kennedy et al. [47] was used. SCS is a syndrome similar to motion sickness, often encountered in simulator or immersive environments, akin to what sailors experience at sea [48]. The SSQ includes 16 symptoms (listed in Supplement IV, Table 1) and primarily captures physiological discomfort and autonomic nervous system activation. Each symptom in the SSQ is rated on a four-point scale: 0 (''none''), 1 (''slight''), 2 (''moderate''), and 3 (''severe''). The symptoms are categorised into three subscales – Nausea (N), Oculomotor Disturbances (O), and Dis-orientation (D) – as well as an overall Total Severity Score (TS). Some symptoms contribute to multiple subscales; for instance, ''Difficulty focusing'' is included in both the ''oculomotor'' and ''disorientation'' categories. Subscale scores are calculated by summing the symptom ratings within each category and multiplying by particular weights: 9.54 for Nausea (range: 0–200.34), 13.92 for Disorientation (range: 0–292.32), and 7.58 for Oculomotor Disturbance (range: 0–159.18). Rather than a simple sum of raw scores, this weighted scoring system, constructed by Kennedy et al. [47], offers a more accurate and nuanced measure of overall SCS, as it accounts for the varying severity levels across its three subscales. The total symptom score is obtained by summing all 16 symptom ratings and multiplying the result by 3.74, yielding an overall SSQ score ranging from 0 to 179.52.

4.3. Test in simulation

The experimental test began with a training session. Participants were first provided with a concise 5-minute tutorial on the interface. The experiment mentor then demonstrated how the 6DoF functionalities of the WING system could be employed to control A-UAVs via the AITL-WING-HITL platform. Two key scenarios were demonstrated to clarify the experiment's objectives: (1) what occurs when neither the human operator nor the system intervenes, resulting in a collision; and (2) how the AITL-WING-HITL platform autonomously responds to impending, probable, and imminent collision risks using a minimum-deviation strategy. These scenarios were illustrated using two 7-minute recorded videos, ''01_No-intervention-no-CA.wmv'' and ''02_

Table 7
Statistical significance test of deviation comparisons using one-tailed dependent T-test for paired samples: Comparison of the episodes within the scenarios to conclude if the learning, improvement and adaptation are statistically significant.

Scenario	Episode	Average dev diff (metre)	# of improvement	Sample size (n)	Average of differences	Significance level (α):	SD of differences	*P*-value		Statistical significance	Fig.
I	I–II	−2314	18	23	−100.6087	0.01	126.7706	0.0009667	$p < 0.01$	Significant	18(a)
II	III–IV	−633	14	23	−27.5217	0.01	183.5751	0.4797	$p > 0.01$	NOT significant	18(b)
III	V–VI	−813	13	23	−35.3478	0.01	176.0255	0.346	$p > 0.01$	NOT significant	18(c)

No-intervention-with-CA.wmv", available in [49]. Following the demonstration, participants engaged in a 7-minute hands-on practice session with support from the experimenter. During this session, they freely explored the platform's functionalities to assess how quickly they could adapt. It was emphasised that the primary objective throughout the episodes was to avoid collisions using the fewest possible manoeuvres via the WING system. In essence, participants were expected to complete each CA task by safely and minimally deviating from the original flight path. Participants were instructed to execute CA manoeuvres outside the ICTZone for safety, but as close as possible to it for efficiency — ideally within the PCTZone. They were also required to avoid creating any new collision risks with other nearby aerial vehicles while evading imminent collisions. A collision during any episode was considered a failure, requiring the participant to repeat that episode without interruption. Three challenging collision-avoidance tasks were assigned, each involving potential conflicts with other aerial vehicles. These three scenarios were repeated once, resulting in a total of six episodes. The repetition allowed for measuring user progress between the first and second attempts. Once participants were familiarised with all system setups, the independent experimental sessions were conducted. Participants were fully immersed in a simulated aerial environment through the WING interface. Given that latency in visual feedback can significantly impair haptic task performance [50,51], our application provided real-time visual updates of both the WING's actions and the environmental interactions (SSA) with other flights. This ensured high transparency, enabling users to properly immerse themselves in the remote environment and promptly correct any un-desirable actions. Each participant completed the six episodes over 42 min, as previously described. For four participants, the test duration increased by seven minutes due to episode failures requiring repetition: two participants from the non-experienced student group in Episode 3, one from the non-experienced staff group in Episode 3, and one from the experienced staff group in Episode 5. All system-generated data produced by participants during the simulation were recorded for subsequent performance evaluation and statistical comparison.

Each participant was able to visually interact with specific A-UAVs and manipulate their navigation and trajectories in relation to nearby flights, with the goal of successfully completing the task without collisions and maximising task performance. All participants began with the first episode and proceeded sequentially through the second, third, fourth, fifth, and sixth episodes without interruption. The experiment concluded with the completion of post-test questionnaires. Upon finishing all six episodes, participants were asked to complete the SSQ and a function-specific evaluation – the OQQ – as previously described. These instruments were used to assess overall user experience and system effectiveness from multiple perspectives. In addition to the questionnaire data, system-generated records from each episode were analysed to evaluate both individual participant performance and overall system functionality. These records included: (i) the time taken to successfully complete each episode (e.g. time required for the HTM to resolve specific problems); (ii) the deviation distance from the original planned trajectory; and (iii) the number of failures, such as imminent collision alarms or actual collisions. The following sections provide detailed elaboration of the scenarios used in the experiment.

4.3.1. The first scenario within the first two episodes

The platform's autonomous response to imminent collision risks using a minimum deviation strategy was demonstrated in the video titled "02_No-intervention-with-CA.wmv". Participants were expected to replicate similar manoeuvres during the first two episodes, specifically within the PCTZone. Entering the ICTZone significantly increases the risk of collision and is considered a weakness in participant performance. Any actual collision was classified as a failure, requiring the repetition of the episode. Upon entering the PCTZone, participants had a window of 3 s to reach the ICTZone, and up to 6 s before a collision would occur if no corrective action was taken. Participant performance was evaluated by comparing their manoeuvres to both the system's benchmark trajectory demonstrated in "02_No-intervention-with-CA.wmv" and to one another, primarily based on the deviation from the original flight path. To ensure the measurement of participants' unassisted performance, the full-control (master–slave) intervention mode (Fig. 15) was employed. This configuration prevents the system from initiating any autonomous manoeuvres during imminent collision risks or actual collisions. Thus, the assessment reflects purely the participants' capabilities without system interference. For an illustrative example of the manoeuvres expected in the first two episodes, readers are referred to the video titled "FirstScenario.wmv" in [49].

4.3.2. The second scenario within the third and fourth episodes

In this scenario, the co-activity (shared) intervention mode (Fig. 15) was employed. Participants were expected to perform vertical manoeuvres – either upward or downward – based on the altitudes and velocities of nearby flights posing collision risks. Entering the ICTZone significantly increases the likelihood of a collision, and if the system triggers an autonomous manoeuvre to avoid an imminent collision, the episode is considered a failure and must be repeated. Participants had a 3-second window to reach the ICTZone after entering the PCTZone, within which autonomous interventions are activated. Participant performance was evaluated by comparing their trajectories to the system's benchmark manoeuvre (i.e. "02_No-intervention-with-CA.wmv"), as well as against one another, with particular attention to the deviation from the original trajectory.

4.3.3. The third scenario within the last two episodes

In the third and fourth episodes, participants were expected to per-form directional manoeuvres opposite to the detected threat: ascending when the potential collision path involved a descending trajectory, and descending when the collision threat came from below. The co-activity (shared) intervention mode (Fig. 15) was employed for this scenario. Entering the ICTZone significantly increased the risk of collision, and any autonomous manoeuvre initiated by the system to prevent an imminent collision was considered a failure, requiring the episode to be repeated. Upon entering the PCTZone, participants had a 3-second window to respond before the ICTZone threshold was reached and autonomous actions were triggered. Participant performance was assessed by comparing their manoeuvres against the system's benchmark (i.e. "02_No-intervention-with-CA.wmv") and against one another, with a focus on the deviation from the original flight trajectory.

5. Experimental results

A dependent t-test for paired samples was conducted to evaluate the outcomes of the quantitative data collected during the experiment. The analysis was performed with a statistical significance level corresponding to a 99% confidence interval. A detailed summary of the experimental results is provided in Supplement V to facilitate further analysis and enable researchers to draw broader conclusions. The key findings from these results are outlined below.

5.1. Results: System-generated recordings

The summarised deviation results, autonomously recorded by the system during the experiments, are presented in Supplement V (Ta-ble 1). As shown in Table 7, which presents averaged data from Figs. 18(a), 18(b), and 18(c), Scenario I demonstrates a statistically significant improvement from Episode I to Episode II. In contrast, Scenarios II (Episodes III to IV) and III (Episodes V to VI) exhibit only minor, statistically insignificant improvements (i.e. 28 m and 35 m, respectively). A total of 18 out of 23 participants improved their performance in Scenario I, whereas only 14 participants improved in Scenarios II and III. This suggests that Scenarios II and III may require additional training for participants to achieve more substantial performance gains. These scenarios likely impose a higher cognitive load, as they demand greater attention to the real-time Situation Awareness (SA) and navigation data generated by the system. This increased demand may be attributed in part to the cognitive limitations associated with interpreting such information via the 2D GUI of the AITL-WING-HITL platform. Fig. 18(d) visualises the average deviation across all scenarios and episodes relative to the benchmark value – the Minimum Expected Deviation Level (MEDL) – recorded in the autonomous mode (i.e. 730 m). This visualisation highlights the relative differences in performance, both between participants and in comparison with the autonomous system. Participant performance is considered more favourable the closer the deviation is to the MEDL. Participant adaptation appears to be more effective in Scenario I, with the deviation in Episode II decreasing to 837 m – approaching the MEDL – likely due to the reduced cognitive load. In Episode I of Scenario I, where participants first began engaging with the WING and the interface, the deviation was higher (938 m), which is expected due to the initial learning curve. In comparison, the first episodes of Scenarios II and III yielded slightly smaller deviations (920 m and 924 m, respectively), likely due to prior exposure. How-ever, subsequent improvements in Scenarios II and III were minimal (892 m and 889 m, respectively), indicating that additional exposure alone may not be sufficient for significant performance enhancement in tasks involving greater cognitive complexity.

From a broader perspective, the classification of average deviation values across participant groups is visualised in Fig. 19, based on the detailed data provided in Supplement V (Table 1). The group-specific analyses are summarised below:

– Scenario I: All participant groups demonstrated performance improvements from Episode I to Episode II, with respective improvement values of 30 m, 172 m, 108 m, and 47 m. While it was expected that the expert group would perform best when engaging with the WING platform, the results indicate that both prior experience and familiarity with similar systems play a significant role in enhancing performance. The experienced staff group outperformed the others, achieving deviation values of 815 m in Episode I and 785 m in Episode II. Notably, the non-experienced staff showed the greatest improvement, reducing their deviation by 172 m. It is important to note that achieving improvements becomes increasingly difficult as performance approaches the MEDL, due to the elevated risk of collision. In this context, the experienced staff's relatively modest improvement of 30 m is reasonable. Interestingly, the non-experienced students performed better than the experienced students, with deviation values of 840 m and 793 m, compared to 957 m and 849 m, respectively.

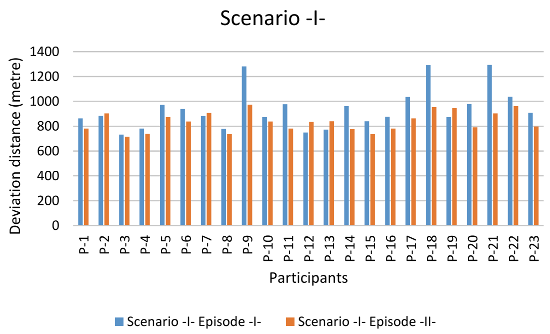

(a) Results for the first scenario: Improvement for 18 participants

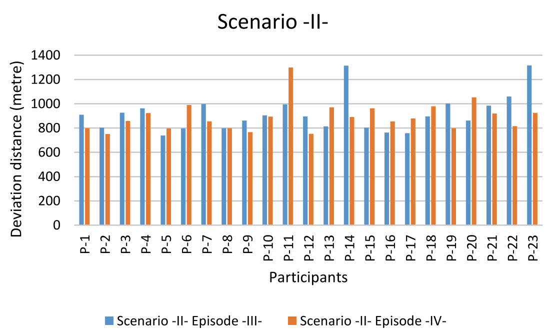

(b) Results for the second scenario: Improvement for 14 participants

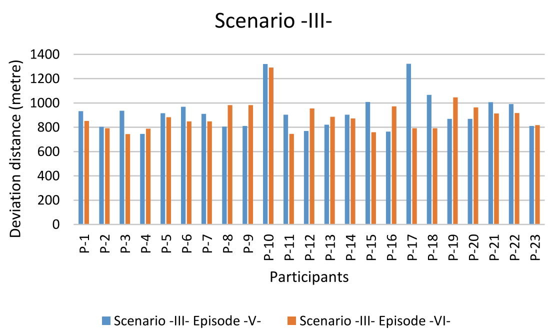

(c) Results for the third scenario: Improvement for 14 participants

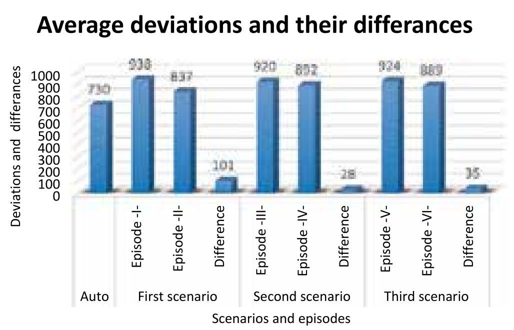

(d) Average results for the scenarios per participant (Figs. 18a, 18b, 18c). "Auto" indicates the minimum expected deviation level (MEDL) that is expected by the autonomous mode to avoid collision risks.

Fig. 18. Graphical presentation of the results obtained from the scenarios elaborated in Supplement–V (Table 1).

– Scenario II: All groups, with the exception of the experienced students (–44 m), improved their performance from Episode III to Episode IV, with improvement values of 68 m, 73 m, and 32 m. Although the experienced students initially outperformed the other groups with a deviation of 870 m in Episode III, their performance declined in Episode IV, with a deviation of 940 m. In contrast, the non-experienced staff again achieved the highest improvement (73 m), demonstrating consistent learning and adaptation.

– Scenario III: All groups improved their performance from Episode V to Episode VI, except for the non-experienced student group, which showed a performance decline (–36 m). The most notable improvement was again observed in the non-experienced staff group, with a deviation reduction of 99 m. The experienced staff group maintained the best overall performance, with deviations of 854 m in Episode V and 794 m in Episode VI, while the non-experienced staff demonstrated the largest performance gain in this scenario.

5.2. Results: Simulation sickness questionnaire

The computation of SSQ scores based on reported symptoms is detailed in Supplement IV (Table 1). While some studies (e.g. [52–54]) suggest that the severity of SS symptoms increases over time, others (e.g. [55]) argue that symptoms tend to decrease with continued inter-action with the system. Given these conflicting findings, the detailed SSQ results from this study are provided in Supplement V (Table 2). Fig. 20 presents the overall SSQ summary scores, including the TS and subscale scores. The total SS score increased from 38.38 at the beginning of the experiment to 42.93 after the training phase, and further to 53.5 by the end of the experiment. The increase from the start to the training phase was not statistically significant, whereas the increase from the training phase to the completion of all scenarios was significant ($p < 0.01$). Nausea (N) and Oculomotor (O) scores showed a slight, statistically insignificant decrease following the training phase and a slight, statistically insignificant increase by the end of the experiment ($p > 0.01$ in both cases). In contrast, Disorientation (D) scores showed a consistent and statistically significant increase across all three phases, rising from 62.34 at the beginning to 68.99 after training and reaching 93.20 by the end of the experiment ($p < 0.01$). It is important to note that even at the final measurement, the disorientation scores remained well below the maximum possible value of 292.32 (as shown in Supplement IV, Table 1).

Participant group SSQ scores are illustrated in Fig. 21, where symptoms – Nausea (N), Oculomotor (O), and Disorientation (D) – are combined to compare differences across groups, and in Fig. 22, where scores are grouped by experimental phase (start, training, and end) to highlight trends per symptom. As shown in Fig. 21, there was no noticeable increase in SSQ scores for the experienced staff across the experiment phases (i.e. 28.99, 26.18, 28.05). In contrast, a consistent and significant increase was observed for both the non-experienced staff (i.e. 37.4, 49.15,

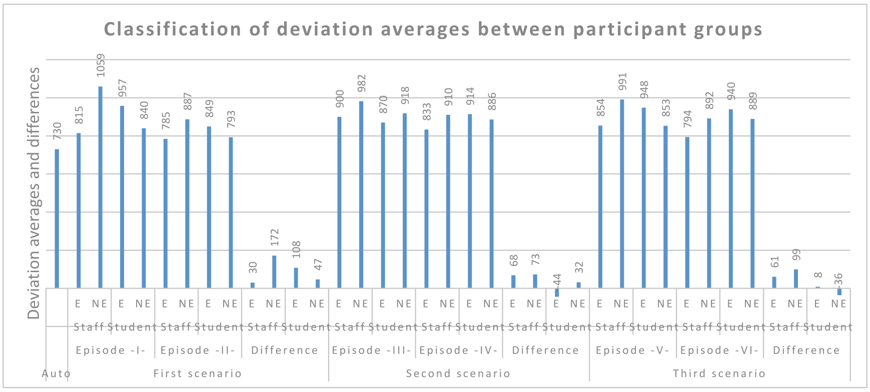

Fig. 19. Classification of deviation averages between participant groups (Supplement-V (Table 1)).

Fig. 20. General scores of the SSQ regarding total SS (TS) and sub class syndromes (Supplement IV (Table 1)).

58.77) and non-experienced students (i.e. 44.88, 50.12, 61.34) from the beginning to the end of the experiment. Al-though the training phase was designed to alleviate simulator sickness symptoms, it instead resulted in a significant increase in scores for the non-experienced staff (49.15) and non-experienced students (50.12). In contrast, the decrease in SSQ scores for the experienced staff (26.18) and experienced students (41.14) during the training phase was not statistically significant. Among all groups, the experienced staff consis-tently reported the lowest SS levels. In Fig. 22, while the experienced staff did not show a significant increase in total SSQ scores over time, the disorientation (D) subscale did increase significantly – from 38.28 to 45.24 – during the experiment. This increase is masked in the overall total due to decreases in the (N) and (O) subscales, which dropped to 16.69 and 24.63, respectively, compared to their initial values (N: 23.85, O: 37.9). The (D) symptom increased significantly across all participant groups. The (N) subscale decreased significantly for the experienced staff but increased for all other groups except the experienced students. The (O) subscale decreased significantly for the experienced staff and both student groups, but increased for the non-experienced staff from the start to the end of the experiment.

5.3. Results: Overall quality questionnaire

The OQQ is provided in Supplement IV (Table 2). Detailed results obtained from the OQQ are presented in Supplement V and summarised in Fig. 23 by question order, in Fig. 24 by score ranking, and in Fig. 25 by participant subgroup. The overall average score across all questionnaire items is 3.9 out of 5. Question Q-5 (“Manoeuvring left/right is easy to implement with the WING”) received the highest approval rating, with an average score of 4.7. In contrast, question Q-16 (“I found the overall AITL-WING-HITL interface as well as the WING easy to use and scalable to support a single HTM controlling more than one A-UAV synchronously”) received the lowest score, averaging 3.4. Questions Q-5, Q-12, Q-11, Q-10, Q-4, and Q-13 were all rated highly, each scoring above 4 out of 5. Regarding participant subgroups (Fig. 25), the experienced staff group provided the highest overall rating, with an average score of 4.29. Conversely, the non-experienced student group gave the lowest ratings, with an average score of 3.67. The non-experienced staff and experienced student groups gave similar ratings (3.90 and 3.88, respectively). Notably, the experienced staff group scored highest across all questionnaire categories. The immersive capabilities of the WING in simulation environments were found to be highly effective. Participants reported that the AITL-WING-HITL platform, in conjunction with the WING, met most of their expectations in manipulating A-UAVs. The responsiveness of the A-UAVs was considered highly satisfactory, particularly in terms of translating the WING’s discrete microstructural inputs into desired task-oriented outputs — such as trajectory adjustments, manoeuvres, velocity, altitude, and heading. Overall, participants responded positively to remote manipulation of A-UAVs in scenarios involving pending, probable, or imminent collision risks using the WING’s 6DoF functionality. Notably, 16 out of 23 participants – 7 of whom were experienced – expressed a preference for using the WING over traditional joysticks (Q-24 in Supplement V, Table 3). QoE can be assessed through measurable QoS parameters; a decline in QoS typically results in reduced QoE [56]. In this context, the immersive quality, comfort, and overall usability of the AITL-WING-HITL platform and the integrated WING were all rated highly. No significant effects of system latency were observed on task performance or responsiveness, indicating a high level of transparency in the simulation environment and, consequently, a high QoE. Based on participant feedback, the primary concerns and additional features to be considered for future integration into the system are outlined as follows.

– Executing manoeuvres above or below other vehicles requires close attention to real-time flight parameters – especially altitude –since discerning vertical separation between vehicles can be challenging in the platform's 2D interactive interface (Fig. 17). This is particularly problematic when aircraft converge at similar latitude and longitude coordinates.

– Experienced participants, familiar with 3D simulation environments, recommended the development of a 3D visualisation mode for the platform to enhance spatial awareness.

– Manipulating vehicle trajectories along the *Z*-axis using the WING could be made more intuitive and functional, particularly when discrete altitude changes are needed – especially in the downward (Z-negative) direction of the device.

– The platform could assist users by suggesting optimal manoeuvring actions (e.g. "descend 50 m", "turn 15◦ left") based on real-time SSA and nearby aircraft data, as it already does for scenarios involving probable or imminent collision risks. Such features may help reduce cognitive load.

6. Challenges

(i) Latencies in wireless communication between A-UAVs and HTMs are a clear limitation, hindering the development of highly transparent DT systems. From a broader perspective, time-varying delays are inevitable during collaborative operations – arising from communication lag, decision-making delays affecting the QoE of HTMs, the processing of large volumes of sensor data, and actuation delays. To enable effective telemanipulation of aerial robots – especially for CA – it is essential to develop transparent systems equipped with estimation-based predictive displays and directional aids (Figs. 9,10) that compensate for these latencies. Further studies on transparent systems, in particular, building the transparency standards, such as IEEE Std 7001-2021 [57], are of prime importance, considering the autonomous systems.

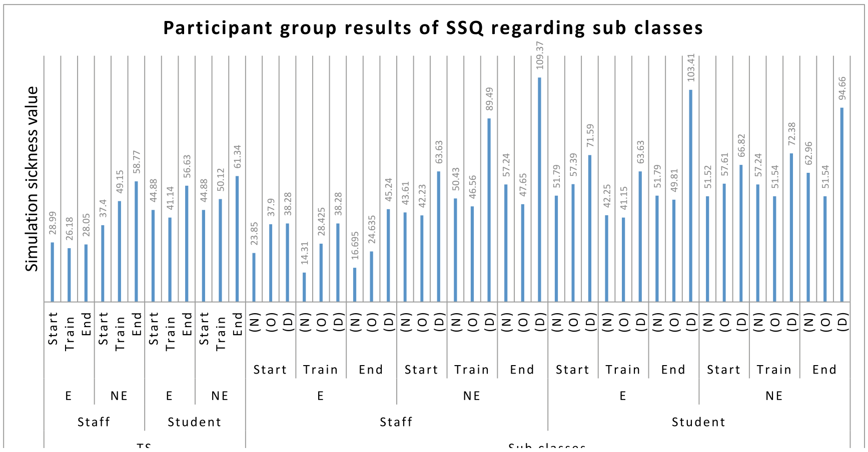

Fig. 21. Participant group scores of SSQ regarding total SS (TS) and SS results with sub classes (Supplement V (Table 2)). The symptoms ((N), (O), (D)) are brought together to perceive the difference from each other.

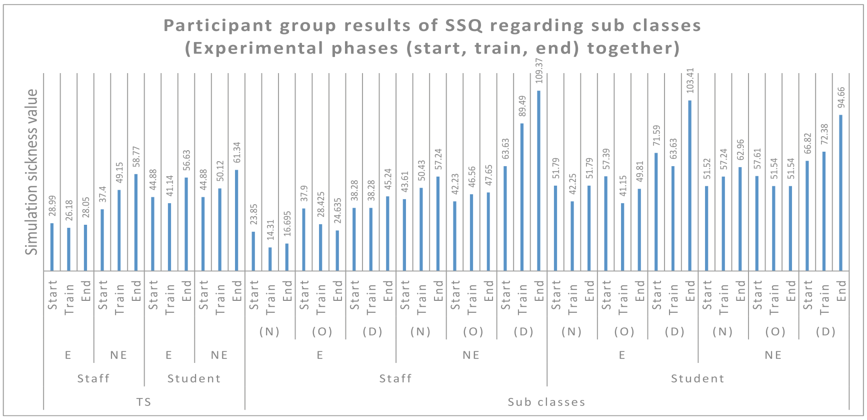

Fig. 22. Participant group scores of SSQ regarding total SS (TS) and SS results with sub classes (Supplement V (Table 2)). Experimental phases (start, train, end) are brought together to perceive the trend per symptom.

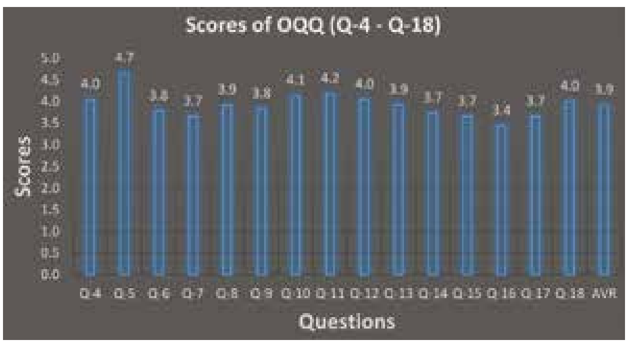

Fig. 23. Scores of OQQ (Q-4 – Q-18) (Supplement V (Table 3)).

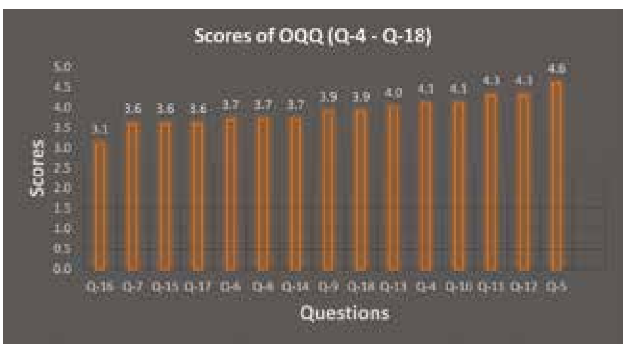

Fig. 24. Sorted scores of OQQ (Q-4 – Q-18) (Supplement V (Table 3)).

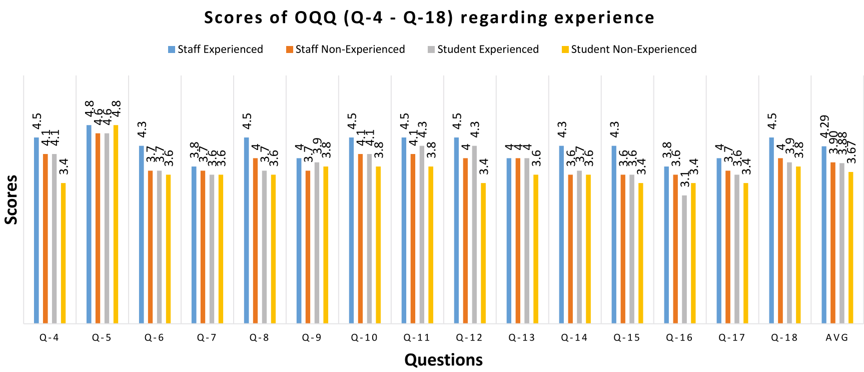

Fig. 25. Scores of OQQ (Q-4–Q-18) (Supplement V (Table 3)) regarding participant sub-groups.

(ii) Malicious interference poses significant threat. A nearby radio transmitter can readily initiate a denial-of-service attack – e.g. via jamming – with reaction times on the order of tens of microseconds, significantly increasing packet loss rates in Vehicle-to-Vehicle (V2V) communication, as demonstrated in multiple studies [58–60]. Additionally, false data injections may occur, highlighting the need for robust authentication mechanisms to validate all inputs [7]. Given these risks, cybersecurity must be treated as a primary concern well in advance of the widespread deployment of telemanipulated A-UAV systems.

(iii Determining optimal obstacle-free trajectories for drones is a complex challenge, constrained by factors such as airspace structure, communication coverage, battery limitations, collision risk, and terrain avoidance [61]. All these constraints must be thoroughly considered in the design of telemanipulation approaches for A-UAV platforms.

7. Lessons learned

(i) 3D interface development for DT systems – excluding extraneous information – can substantially reduce cognitive load during telemanipulation, enhancing operator effectiveness and situational awareness.

(ii) Even with high-quality SA information, effective human telemanipulation remains highly dependent on the cognitive, perceptual, and motor abilities of HTMs, including spatial orientation skills [8]. To mitigate risks from erroneous decisions, it is critical to leverage local intelligence (i.e. AITL) at the remote site (Fig. 15).

(iii) Many drone operations can benefit from a unified framework that facilitates coordinated access to integrated airspace and efficient routing to task locations [62]. The development of robust telemanipulation platforms, as investigated in this study, supports the realisation of such frameworks.

(iv) A major challenge in non-fault-tolerant and non-delay-tolerant telemanipulation of AVs lies in the requirement for real-time intervention with high perceptual awareness and minimal latency (i.e. rapid action-response capability) [8]. A human–teleoperator interface with low cognitive demand can streamline interaction and ensure compatibility with real-world AV capabilities [8]. Future systems must in-corporate advanced, safety-critical interface functionalities, supported by cutting-edge communication infrastructure and analytical tools, to enable tight, time-sensitive coupling between the cyber domain of HTMs and the physical domain of AVs [8]. This research focused on developing such a platform – designed to reduce cognitive load and support one-to-many A-UAV telemanipulation – by leveraging high-functionality coupling tools like the WING and interfaces such as AITL-WING-HITL.

8. Discussion

FA-UAVs are expected to execute their missions with minimal to no human intervention. However, in complex, real-world environments – particularly when multiple UAV missions are conducted by various organisations within a shared, integrated aerospace alongside manned aircraft – unforeseen situations may arise that exceed the autonomous capabilities of A-UAVs. The integration of A-UAVs into broader traffic management systems necessitates the use of coordinated platforms that support collective movement, ensuring safe and efficient mission execution while mitigating mid-air collision risks, as detailed in [42]. Such platforms foster the necessary cohesion to maintain safe separation distances between aerial vehicles. The HOTL and HITL paradigms remain vital in the operation of AVs. Despite decades of research and recent advancements by the tech industry and academia, significant gaps persist in AV capabilities [63]. Addressing unexpected issues remotely, through vehicle teleoperation (i.e. remote driving, manipulation, or control), is therefore critical — both for ensuring public safety and mitigating potential cybersecurity threats [8]. This research aimed to develop an integrated, collaborative approach that enables humans and intelligent drones to co-work in resolving operational challenges (e.g. CA, mission-specific task execution). The proposed platform –AITL-WING-HITL – was designed to provide HTMs with comprehensive monitoring of aerial traffic and direct manipulation capabilities over A-UAVs through advanced intervention tools. Central to this platform is the WING – a force-sensitive, precision control device that facilitates immersive, multi-modal interaction. By enabling a high level of synergistic collaboration between human operators and A-UAVs, the WING ensures effective task execution through an intelligent and responsive interface.

The AITL-WING-HITL platform was evaluated through participant testing using measurable parameters to identify areas for further improvement in the developed interface and techniques, as outlined in Section 4. The outcomes – derived from system-generated recordings, Kennedy's SSQ, and the OQQ – are presented in Section 5, supported by figures, tables, and detailed analyses of group performances. Overall, participants found the platform easy to use, particularly highlighting the high functionality of the WING. This conclusion is based on participant feedback, analysis of user experiences, and preliminary quantitative results gathered during the experimental sessions. While two participants expressed dissatisfaction with the placement of certain interface elements, efficient interactions were generally observed when using the WING. Participants were able to generate trajectories closely aligned with the ideal data set (i.e. MEDL), which was created by the AITL system as a benchmark based on the most optimal trajectories. These results support the conclusion that the trajectory data sets produced by participants using the WING are efficient, and that users can collaboratively and coactively telemanipulate A-UAVs to achieve near-optimal mission outcomes using this intuitive and deployable device. Furthermore, the trajectory waypoints, speeds, and azimuth angles obtained from AITL–HITL co-activity highlight the WING's ease of implementation and manipulation in a practical and effective manner. Additionally, four participants remarked that a wireless version of the WING would enhance user immersion by allowing more freedom of movement within the DT environments of aerial traffic.

The experimental results validate the effectiveness of the proposed AITL-WING-HITL architecture. The WING enables HTMs to perform omnidirectional control in telemanipulating A-UAVs. By combining translational and rotational movements, the WING facilitates the generation of multiple DoFs and functions, allowing users to accomplish highly complex tasks through varied input combinations. The frame-work, with its robust capabilities, is scalable to accommodate multiple A-UAVs operating within mixed aerial traffic environments. Through its immersive system design and synchronous communication features, AITL-WING-HITL enables a single HTM to simultaneously manipulate multiple A-UAVs, even under uncertain, unstructured, and dynamic conditions. This research demonstrates that the proposed framework enhances HTM effectiveness by integrating AITL and HITL co-activity, supporting a wide range of automated, user-friendly functions along-side high-fidelity telepresence and telemanipulation capabilities. More-over, the results indicate that most participants adapted to the platform with ease, requiring minimal training. The AITL-WING-HITL system is highly flexible, addressing the complex, multidimensional dynamics inherent in A-UAV operations. However, based on the analysis of results from Scenarios II and III – compared to Scenario I – participants' perceptual accuracy showed a slight decline due to increased cognitive load. This was particularly evident when generating manoeuvring trajectories that required flying over or under other vehicles, where altitude differences were difficult to perceive in the platform's 2D interactive environment. These findings highlight the potential benefits of 3D telemanipulation interfaces in enhancing the spatial awareness of HTMs. Accordingly, the integration of 3D visual content is identified as a key direction for future development (Section 10). Overall, the experimental design and findings presented in this study offer valuable insights for researchers and developers engaged in similar efforts within the field of remote aerial vehicle manipulation.

9. Limitations of the system

Changes in heart rate, respiration rate, and central nervous system activity are key physiological indicators associated with SCS. Therefore, automatically monitoring these parameters – such as through Electroen-cephalography (EEG) and Electrocardiography (ECG) – could provide a more comprehensive and objective assessment. This approach may offer deeper insights into the onset and progression of SCS symptoms, potentially yielding more accurate and less biased results compared to self-reports. Numerous studies, including those by Dumaska et al. [46], have demonstrated a strong correlation between these physiological indicators and SCS. Additionally, the participant pool in our study comprised 23 individuals – 7 short of our target of 30 – which limited the breadth of our evaluation. Nonetheless, the results obtained from the experiment offered meaningful insights and demonstrated statistical significance in key findings.

10. Conclusion and future work

This research investigates the collaboration between human cognition and machine intelligence through the development of a synergistic collective platform – AITL-WING-HITL – which integrates several sub-systems into a unified architecture (Fig. 2). This architecture generates DTs of aerial traffic and incorporates an immersive control device –the WING (Section 3.1.1) – to enable HTMs to seamlessly interact with and manipulate A-UAVs within mixed aerial traffic environments. The AITL-WING-HITL platform allows HTMs to switch between: (i) inter-vention modes, ranging from no-control (supervisory) to full-control (master–slave) teleoperation (Fig. 15), and (ii) motion modes, including translational motion (x, v, z) and rotational orientation (Ψ, Θ, Φ) (Fig. 4), depending on the required manipulation task. Using the WING with 6DoF, the platform enables the remote extension of human expertise, offering HTMs the ability to telemanipulate A-UAVs with a high degree of precision and flexibility across various intervention modes. This capability supports: (i) achieving high levels of task performance, and (ii) ensuring that A-UAVs exhibit reliable autonomous behaviour under unanticipated conditions – both critical for maintaining aerial and ground safety. The system was evaluated in a range of simulated laboratory scenarios involving both experienced and inexperienced participants to assess platform functionality and the effectiveness of the WING in telemanipulating A-UAVs. Results indicate that teleimpedance manipulation via the WING is effective: participants were able to modulate hand impedance appropriately – that is, applying and releasing hand forces with precise timing – to perform the required actuation tasks successfully. The key outcomes of this research are summarised as follows:

– The WING, integrated within the AITL-WING-HITL platform, provides HTMs with finely tuned, tightly coupled control of A-UAVs by translating its discrete microstructural signals directly into task-oriented actions with high responsiveness.

– The WING's dexterous force-generation capability, combined with strong spatial, cognitive, and ergonomic features and minimal training requirements, enables efficient centralised telemanipulation of decentralised A-UAVs within the AITL-WING-HITL architecture, resulting in high task performance.

– The co-work and co-activity mechanisms between HTMs and A-UAVs, facilitated through the platform's intervention modes – investigated here for the first time specifically in the context of A-UAVs –enable synergistic collaboration. This dual-intelligence system leverages both vehicle-side autonomy and human-side decision-making to achieve complex operational goals through effective human–machine dialogue.

– This research advances the understanding of A-UAV telemanipulation by exploring user immersion and adaptability within the AITL-WING-HITL framework. It provides valuable insights into how A-UAVs can be safely and efficiently manipulated – especially when the autonomous system (AITL agent), acting as the new ‘‘driver’’, encounters situations that exceed its autonomous capabilities.

Scalable systems such as AITL-WING-HITL offer a viable solution to the current limitations of A-UAV usage, enabling their integration into a wide range of applications without having to wait for the perfection of autonomous technologies – a milestone still years away. In the future, complex, time- and safety-critical real-world tasks will be performed coactively by HTMs and AITL-enabled A-UAVs. To enhance HTM perception and cognitive engagement, the current 2D GUI of the AITL-WING-HITL platform is planned to be replaced with a more immersive 3D visual environment. Additionally, key questions remain for future investigation: What is the optimal number of A-UAVs that a single highly skilled HTM can effectively manage? And how many HTMs should be assigned to a given region, city, or country, taking into account factors such as aerial traffic density, A-UAV automation levels, and task-specific assistance needs? These assessments aim to ensure the safe and efficient operation of aerospace systems within an integrated UTM+ATM framework. Another important future direction is the use of reinforcement learning (RL) – including Transfer Learning (TL) [64] and Federated Learning (FL) [65] – to train drones based on insights gained during HTM-led telemanipulation. This approach will help A-UAVs acquire greater autonomy by learning how to act under uncertain conditions. In the long term, our objective is to develop robust systems in which HTMs and A-UAVs collaborate seamlessly to accomplish complex tasks with high levels of performance.

CRediT authorship contribution statement

Kaya Kuru: Writing – review & editing, Writing – original draft, Visualization, Validation, Supervision, Software, Resources, Project ad-ministration, Methodology, Investigation, Funding acquisition, Formal analysis, Data curation, Conceptualization. Sam Worthington: Writing – review & editing, Validation, Resources. Darren Ansell: Validation, Supervision, Resources, Investigation, Funding acquisition. John M. Pinder: Writing – review & editing, Resources, Investigation, Formal analysis. Aadithya Sujit: Writing – review & editing, Resources, Investigation. Benjamin J. Watkinson: Writing – review & editing, Validation, Resources, Formal analysis. Keith Vinning: Writing – review & editing, Resources, Investigation, Data curation. Lee Moore: Writing – review & editing, Resources, Data curation. Chris Gilbert: Writing –review & editing, Resources, Formal analysis. David Jones: Writing –review & editing, Validation, Resources, Investigation. Claire Tinker-Mill: Writing – review & editing, Validation, Supervision, Project ad-ministration, Funding acquisition.

Declaration of competing interest

The authors declare that they have no known competing financial interests or personal relationships that could have appeared to influence the work reported in this paper.

Funding, ethics and acknowledgements

This report presents independent research funded by the European Regional Development Fund's (ERDF) business support programme (Project Number: 19R19P03775). The funding agreement guaranteed the authors full independence in the design of the study, data interpretation, and the writing and publication of this report. The views expressed herein are those of the authors and do not necessarily reflect those of the funder. This research was conducted with ethical approval from the University of Lancashire (Science Ethics Review Panel Reference: SCIENCE 01031). The authors extend their sincere thanks to all participants who volunteered for the experiment, as well as to the anonymous reviewers for their valuable feedback and constructive suggestions.

Appendix A. Supplementary data

Supplementary material related to this article can be found online at https://doi.org/10.1016/j.robot.2026.105486.

Data availability

Data will be made available on request.

References

[1] NewYorkTimes, A successful exhibition of electrical transmission without wires in the garden, 1898.

[2] T.K. Sarkar, R. Mailloux, A.A. Oliner, M. Salazar-Palma, D.L. Sengupta, History of Wireless, Wiley, NJ, USA, 2006.

[3] N. Tesla, Method of and apparatus for controlling mechanism of moving vessels or vehicles, 1898, U.S. Patent US613809A.

[4] J. Turi, Tesla's toy boat: A drone before its time, 2014.

[5] K. Kuru, D. Ansell, W. Khan, H. Yetgin, Analysis and optimization of unmanned aerial vehicle swarms in logistics: An intelligent delivery platform, IEEE Access 7 (2019) 15804–15831, http://dx.doi.org/10.1109/ACCESS.2019.2892716.

[6] K. Kuru, W. Khan, A framework for the synergistic integration of fully au-tonomous ground vehicles with smart city, IEEE Access 9 (2021) 923–948, http://dx.doi.org/10.1109/ACCESS.2020.3046999.

[7] K. Kuru, Planning the future of smart cities with swarms of fully autonomous unmanned aerial vehicles using a novel framework, IEEE Access 9 (2021) 6571–6595, http://dx.doi.org/10.1109/ACCESS.2020.3049094.

[8] K. Kuru, Conceptualisation of human-on-the-loop haptic teleoperation with fully autonomous self-driving vehicles in the urban environment, IEEE Open J. Intell. Transp. Syst. 2 (2021) 448–469, http://dx.doi.org/10.1109/OJITS.2021.3132725.

[9] J.M. Bradshaw, V. Dignum, C. Jonker, M. Sierhuis, Human-agent-robot team-work, IEEE Intell. Syst. 27 (2) (2012) 8–13, http://dx.doi.org/10.1109/MIS.2012. 37.

[10] M. Chowdhury, M. Maier, Toward dynamic hart-centric task offloading over fiwi infrastructures in the tactile internet era, IEEE Commun. Mag. 57 (11) (2019) 123–128, http://dx.doi.org/10.1109/MCOM.001.1800669.

[11] Y. Li, Trends in control and decision-making for human–robot collaboration systems [bookshelf], IEEE Control Syst. Mag. 39 (2) (2019) 101–103, http: //dx.doi.org/10.1109/MCS.2018.2888714.

[12] M. Shahbazi, S.F. Atashzar, R.V. Patel, A systematic review of multilateral teleoperation systems, IEEE Trans. Haptics 11 (3) (2018) 338–356, http://dx.doi.org/10.1109/TOH.2018.2818134.

[13] W.R. Ferrell, T.B. Sheridan, Supervisory control of remote manipulation, IEEE Spectr. 4 (10) (1967) 81–88, http://dx.doi.org/10.1109/MSPEC.1967.5217126.

[14] K. Kuru, Trustfsdv: Framework for building and maintaining trust in self-driving vehicles, IEEE Access 10 (2022) 82814–82833, http://dx.doi.org/10. 1109/ACCESS.2022.3196941.

[15] V.R. Garate, S. Gholami, A. Ajoudani, A scalable framework for multi-robot tele-impedance control, IEEE Trans. Robotics 37 (6) (2021) 2052–2066, http: //dx.doi.org/10.1109/TRO.2021.3071530.

[16] Y. Nakauchi, T. Okada, N. Yamasaki, Y. Anzai, Multi-agent interface archi-tecture for human–robot cooperation, in: Proceedings 1992 IEEE International Conference on Robotics and Automation, Vol. 3, 1992, pp. 2786–2788, http: //dx.doi.org/10.1109/ROBOT.1992.220012.

[17] T. Laengle, T. Hoeniger, L. Zhu, Cooperation in human–robot-teams, in: ISIE'97 Proceeding of the IEEE International Symposium on Industrial Electronics, Vol. 3, 1997, pp. 1297–1301, http://dx.doi.org/10.1109/ISIE.1997.648935.

[18] T. Suzuki, K. Yokota, H. Asama, H. Kaetsu, I. Endo, Cooperation between the human operator and the multi-agent robotic system: evaluation of agent monitoring methods for the human interface system, in: Proceedings 1995 IEEE/RSJ International Conference on Intelligent Robots and Systems. Human Robot Interaction and Cooperative Robots, Vol. 1, 1995, pp. 206–211, http: //dx.doi.org/10.1109/IROS.1995.525798, vol.1.

[19] T. Fujita, H. Kimura, The design of software development system for multiple robots, in: Proceedings of 1993 IEEE/RSJ International Conference on Intelligent Robots and Systems, IROS'93, Vol. 2, 1993, pp. 1119–1125, http://dx.doi.org/ 10.1109/IROS.1993.583331, vol.2.

[20] T. Fong, S. Grange, C. Thorpe, C. Baur, Multi-robot remote driving with collaborative control, in: Proceedings 10th IEEE International Workshop on Robot and Human Interactive Communication. ROMAN 2001 (Cat. No. 01TH8591), 2001, pp. 237–242, http://dx.doi.org/10.1109/ROMAN.2001.981908.

[21] T. Fong, C. Thorpe, C. Baur, Multi-robot remote driving with collaborative control, IEEE Trans. Ind. Electron. 50 (4) (2003) 699–704, http://dx.doi.org/10.1109/TIE.2003.814768.

[22] T.W. Fong, C. Thorpe, C. Baur, Advanced interfaces for vehicle teleoperation: Collaborative control, sensor fusion displays, and remote driving tools, Auton. Robot.: Spec. Issue Teleoperation Interfaces 11 (1) (2001) 77–85.

[23] T.W. Fong, Collaborative Control: A Robot-Centric Model for Vehicle Tele-operation (Ph. D. thesis), Carnegie Mellon University, Pittsburgh, PA, 2001.

[24] I. Nourbakhsh, K. Sycara, M. Koes, M. Yong, M. Lewis, S. Burion, Human–robot teaming for search and rescue, IEEE Pervasive Comput. 4 (1) (2005) 72–79, http://dx.doi.org/10.1109/MPRV.2005.13.

[25] S. Hirche, M. Buss, Human-oriented control for haptic teleoperation, Proc. IEEE 100 (3) (2012) 623–647, http://dx.doi.org/10.1109/JPROC.2011.2175150.

[26] A.K. Mithal, S.A. Douglas, Differences in movement microstructure of the mouse and the finger-controlled isometric joystick, in: Proceedings of the SIGCHI Conference on Human Factors in Computing Systems, CHI'96, Association for Computing Machinery, New York, NY, USA, 1996, pp. 300–307, http://dx.doi.org/10.1145/238386.238533.

[27] M. Martins, A. Cunha, L. Morgado, Usability test of 3dconnexion 3d mice versus keyboard+mouse in second life undertaken by people with motor disabilities due to medullary lesions,

Procedia Comput. Sci. 14 (2012) 119–127, http: //dx.doi.org/10.1016/j.procs.2012.10.014, Proceedings of the 4th International Conference on Software Development for Enhancing Accessibility and Fighting Info-exclusion (DSAI 2012).

[28] M.J. Turner, T. Morris, M. Sandoval, 12DoF Interaction for Scientific Visualisa-tion, in: T.R. Wan, F. Vidal (Eds.), Computer Graphics and Visual Computing, The Eurographics Association, 2017, http://dx.doi.org/10.2312/cgvc.20171274.

[29] M. Sandoval, Multiple Degrees-of-Freedom Input Devices for Interactive Com-mand and Control Within Virtual Reality in Industrial Visualizations (Ph.D. thesis), Department of Computer Science, The University of Manchester, Manchester, UK, 2023.

[30] M. Sandoval, T. Morris, M. Turner, Controlling 3D visualisations with multiple degrees of freedom, in: F.P. Vidal, G.K.L. Tam, J.C. Roberts (Eds.), Computer Graphics and Visual Computing, CGVC, The Eurographics Association, 2019, http://dx.doi.org/10.2312/cgvc.20191263.

[31] R.A. Suárez Fernández, J.L. Sanchez-Lopez, C. Sampedro, H. Bavle, M. Molina, P. Campoy, Natural user interfaces for human-drone multi-modal interaction, in: 2016 International Conference on Unmanned Aircraft Systems, ICUAS, 2016, pp. 1013–1022, http://dx.doi.org/10.1109/ICUAS.2016.7502665.

[32] E. Peshkova, M. Hitz, B. Kaufmann, Natural interaction techniques for an unmanned aerial vehicle system, IEEE Pervasive Comput. 16 (01) (2017) 34–42, http://dx.doi.org/10.1109/MPRV.2017.3.

[33] P. Abtahi, J.L.E.D.Y. Zhao, J.A. Landay, Drone near me: Exploring touch-based human-drone interaction, Proc. ACM Interact. Mob. Wearable Ubiquitous Technol. 1 (3) (2017) http://dx.doi.org/10.1145/3130899.

[34] K. Kuru, H. Yetgin, Transformation to advanced mechatronics systems within new industrial revolution: A novel framework in automation of everything (aoe), IEEE Access 7 (2019) 41395–41415, http://dx.doi.org/10.1109/ACCESS.2019. 2907809.

[35] S. Bouabdallah, M. Becker, R. Siegwart, Autonomous miniature flying robots: coming soon! - research, development, and results, IEEE Robot. Autom. Mag. 14 (3) (2007) 88–98, http://dx.doi.org/10.1109/MRA.2007.901323.

[36] G. Coppin, F. Legras, Autonomy spectrum and performance perception issues in swarm supervisory control, Proc. IEEE 100 (3) (2012) 590–603, http://dx.doi. org/10.1109/JPROC.2011.2174103.

[37] M. Radovic, Tech talk: Untangling the 5 levels of drone autonomy, 2019.

[38] K. Nonami, Present state and future prospect of autonomous control technology for industrial drones, IEEJ Trans. Electr. Electron. Eng. 15 (1) (2020) 6–11, http://dx.doi.org/10.1002/tee.23041, arXiv:https://onlinelibrary.wiley.com/doi/pdf/10.1002/tee.23041.

[39] A. Murray, J. Rhymer, D.G. Sirmon, Humans and technology: Forms of conjoined agency in organizations,

Acad. Manag. Rev. 46 (3) (2021) 552–571, http://dx. doi.org/10.5465/ amr.2019.0186.

[40] M. Anderson, K. Fort, Human where? a new scale defining human involvement in technology communities from an ethical standpoint, Int. Rev. Inf. Ethics 31 (1) (2022).

[41] M. Say, Loti looks at 'humans in the loop' in ai deployments, 2025.

[42] K. Kuru, J.M. Pinder, B.J. Watkinson, D. Ansell, K. Vinning, L. Moore, C. Gilbert, A. Sujit, D. Jones, Toward mid-air collision-free trajectory for au-tonomous and pilot-controlled unmanned aerial vehicles, IEEE Access 11 (2023) 100323–100342, http://dx.doi. org/10.1109/ACCESS.2023.3314504.

[43] R.W. Osborne, Y. Bar-Shalom, P. Willett, G. Baker, Design of an adaptive passive collision warning system for uavs, IEEE Trans. Aerosp. Electron. Syst. 47 (3)(2011) 2169–2189, http://dx. doi.org/10.1109/TAES.2011.5937290.

[44] K. Kuru, Human-in-the-loop telemanipulation schemes for autonomous unmanned aerial systems, in: 2024 4th Interdisciplinary Conference on Electrics and Com-puter, INTCEC, 2024, pp. 1–6, http://dx.doi.org/10.1109/INTCEC61833.2024. 10603071.

[45] N. Amirshirzad, A. Kumru, E. Oztop, Human adaptation to human–robot shared control, IEEE Trans. Hum.–Mach. Syst. 49 (2) (2019) 126–136, http://dx.doi. org/10.1109/ THMS.2018.2884719.

[46] N. Dużmańska, P. Strojny, A. Strojny, Can simulator sickness be avoided? A review on temporal aspects of simulator sickness, 9, 2018, http://dx.doi.org/10. 3389/fpsyg.2018.02132,

[47] R.S. Kennedy, N.E. Lane, K.S. Berbaum, M.G. Lilienthal, Simulator sickness ques-tionnaire: An enhanced method for quantifying simulator sickness, Int. J. Aviat. Psychol. 3 (3) (1993) 203–220, http://dx.doi.org/10.1207/ s15327108ijap0303_3, arXiv:https:// doi.org/10.1207/s15327108ijap0303_3.

[48] K. Brunnström, E. Dima, T. Qureshi, M. Johanson, M. Andersson, M. Sjöström, Latency impact on quality of experience in a virtual reality simulator for remote control of machines, Signal Process., Image Commun. 89 (2020) 116005, http: //dx.doi.org/10.1016/j. image.2020.116005.

[49] K. Kuru, Telemanipulation of autonomous drones using digital twins of aerial traffic, 2024, http://dx.doi.org/10.21227/ kn5m-z290.

[50] C. Jay, M. Glencross, R. Hubbold, Modeling the effects of delayed haptic and vi-sual feedback in a collaborative virtual environment, ACM Trans. Comput.-Hum. Interact. 14 (2) (2007) 8–es, http://dx.doi. org/10.1145/1275511.1275514.

[51] C. Jay, R. Hubbold, Delayed visual and haptic feedback in a reciprocal tapping task, in: First Joint Eurohaptics Conference and Symposium on Haptic Interfaces for Virtual Environment and Teleoperator Systems. World Haptics Conference, 2005, pp. 655–656, http:// dx.doi.org/10.1109/WHC.2005.29.

[52] J.D. Moss, E.R. Muth, Characteristics of head-mounted displays and their effects on simulator sickness, Hum. Factors 53 (3) (2011) 308–319, http://dx.doi.org/ 10.1177/0018720811405196, PMID: 21830515. arXiv:https://doi.org/10.1177/ 0018720811405196.

[53] B.-C. Min, S.-C. Chung, Y.-K. Min, K. Sakamoto, Psychophysiological evaluation of simulator sickness evoked by a graphic simulator, Appl. Ergon. 35 (6) (2004) 549–556, http://dx.doi. org/10.1016/j.apergo.2004.06.002.

[54] J. Lee, M. Kim, J. Kim, A study on immersion and vr sickness in walking interaction for immersive virtual reality applications, Symmetry 9 (5) (2017) http://dx.doi.org/10.3390/sym9050078.

[55] S.V.G. Cobb, S. Nichols, A. Ramsey, J.R. Wilson, Virtual reality-induced symp-toms and effects (vrise), Presence: Teleoper. Virtual Env. 8 (2) (1999) 169–186, http://dx.doi. org/10.1162/105474699566152.

[56] K. Desai, S. Raghuraman, R. Jin, B. Prabhakaran, Qoe studies on interactive 3d teleimmersion, in: 2017 IEEE International Symposium on Multimedia, ISM, 2017, pp. 130–137, http://dx.doi. org/10.1109/ISM.2017.27.

[57] IEEE Standard for Transparency of Autonomous Systems, IEEE Std 7001–2021, 2022, pp. 1–54, http://dx.doi.org/10.1109/ IEEESTD.2022.9726144.

[58] K. Sjoberg, P. Andres, T. Buburuzan, A. Brakemeier, Cooperative intelligent transport systems in Europe: Current deployment status and outlook, IEEE Veh. Technol. Mag. 12 (2) (2017) 89–97.

[59] N. Lyamin, A. Vinel, D. Smely, B. Bellalta, Etsi dcc: Decentralized congestion control in c-its, IEEE Commun. Mag. 56 (12) (2018) 112–118.

[60] O. Punal, C. Pereira, A. Aguiar, J. Gross, Experimental characterization and modeling of rf jamming attacks on vanets, IEEE Trans. Veh. Technol. 64 (2)(2015) 524–540.

[61] S. Sekander, H. Tabassum, E. Hossain, Multi-tier drone architecture for 5g/ b5g cellular networks: Challenges and trends and prospects, IEEE Commun. Mag. 56 (3) (2018) 96–103.

[62] M. Gharibi, R. Boutaba, S.L. Waslander, Internet of drones, IEEE Access 4 (2016) 1148–1162, http://dx.doi.org/10.1109/ACCESS.2016.2537208.

[63] B. Goldfain, P. Drews, C. You, M. Barulic, O. Velev, P. Tsiotras, J.M. Rehg, Autorally: An open platform for aggressive autonomous driving, IEEE Control Syst. Mag. 39 (1) (2019) 26–55, http://dx.doi.org/10.1109/ MCS.2018.2876958.

[64] K. Kuru, Definition of multi-objective deep reinforcement learning reward functions for self-driving vehicles in the urban environment, IEEE Trans. Veh. Technol. 11 (2024) 1–12.

[65] K. Kuru, Management of geo-distributed intelligence: Deep insight as a service (DINSaaS) on forged cloud platforms (FCP), J. Parallel Distrib. Comput. 149 (2021) 103–118, http:// dx.doi.org/10.1016/j.jpdc.2020.11.009.

The paper is originally published in Robotics and Autonomous Systems, Volume 202, 2026.

The paper is republished with authors' permission. https://doi.org/10.1016/j. robot.2026.105486.

Leica CityMapper-3 airborne hybrid system

Leica CityMapper-3 airborne hybrid system is designed to improve operational efficiency by combining the latest imaging and LiDAR technologies within a single, configurable platform, streamlining data acquisition across demanding urban and regional mapping applications. On the imaging side, CityMapper-3 is the first CityMapper to feature a Leica MFC250-based camera system, powered by Sony's IMX811 sensor, delivering up to a 30% increase in acquisition efficiency compared to previous generations. *leica-geosystems.com*

Coastal Observation Research Lab Inaugurated at Andhra University

A state-of-the-art Coastal Observation Research Laboratory (CORAL), funded by the National Remote Sensing Centre (NRSC), was recently inaugurated at the Centre for Studies on Bay of Bengal (CSBoB) at Andhra University, strengthening ocean and climate research in the region. The facility was inaugurated by NRSC director Dr Prakash Chauhan and Andhra University Vice-Chancellor prof. G.P. Raja Sekhar. Established under the NICES CORAL project, the laboratory has received `1.6 crore in funding from the NRSC over three years, while scientific equipment worth nearly `12 crore has been installed.

The laboratory houses advanced instruments, including High-Performance Liquid Chromatography (HPLC), FTIR Spectrophotometer, Dual-Beam UV-VIS Spectrophotometer, pCO_2 Sensor, Coulometer, Sun Photometer, Ozonometer, Nutrient Auto-Analyzer, Flow Cytometer and a Water Purification System. These will enable detailed analysis of dissolved inorganic carbon, nutrients, plankton and dissolved oxygen in ocean waters.

Visakhapatnam was selected for the facility because of its strategic location along the western Bay of Bengal, where river inflows, monsoon variability, cyclone activity and rapidly changing coastal ecosystems make it a natural climate laboratory. The research is expected to improve understanding of carbon cycling, marine ecosystems and aquaculture that supports coastal livelihoods. The NRSC is currently implementing five projects at CSBoB, including the new coastal observation initiative. As part of the project, research cruises will be conducted along selected transects in the Bay of Bengal to study ocean-atmosphere and land-sea interactions and their impact on marine ecosystems. *www.deccanchronicle.com*

100 Percent National LiDAR Coverage of All Low-Lying Islands in Tonga

In a major step toward climate resilience and evidence-based national planning, the Kingdom of Tonga has become one of the very few Pacific Island Countries with comprehensive national LiDAR coverage in 2026. This milestone was delivered through the Tonga Coastal Resilience Project (TCRP), funded by the Green Climate Fund (GCF) and implemented by the United Nations Development Programme (UNDP) in partnership with the Government of Tonga.

With the completion of the 2026 survey, Tonga has establish its first complete national LiDAR baseline to support coastal risk modelling, sea-level rise projections, disaster preparedness, infrastructure planning and long-term climate adaptation.

As part of this effort, a coastal mapping survey was conducted over Tongatapu and Ha'apai island group from 21 March to 18 April 2026 using a specialized survey aircraft. The survey will utilise LiDAR. *www.undp.org*

iXM-FS130 by Phase One

Phase One has announced the iXM-FS130, a next-generation aerial mapping camera designed to unlock sub-centimeter ground sample distance (GSD) missions from a fixed-wing aircraft. It is built on the iXM platform and is introducing Phase One's patented Fusion Shutter™ technology. Designed for fixed-wing aircraft operations, it sets a new performance benchmark for large-scale aerial mapping, corridor inspection, and defense-grade imaging. *phaseone.com*

UAE to boost nation's expertise in space sector

A programme has been announced to enhance Emirati expertise in the space sector. The SEO satellite mission is a collaboration involving the National Space Science and Technology Centre at United Arab Emirates University. The project, developed in co-operation with partners in China, aims to build national capabilities by involving Emirati engineers, researchers and students in all stages of satellite development and operations. The mission provides practical experience through its integrated facilities, including ground stations and satellite assembly, integration and testing, helping to prepare a new generation of specialists to support the growth of the UAE's space sector. *www.thenationalnews.com*

South Korea launches 4th EO satellite from US

South Korea has launched its fourth Earth observation satellite from Vandenberg Space Force Base in California It carries a domestically developed wide-area observation camera capable of imaging the entire Korean Peninsula every three days. It is the country's first satellite dedicated to agriculture and forestry, designed to support applications including crop monitoring, forest management, disaster response and climate analysis. The satellite is scheduled to enter full service in the first half of 2027. *www.aa.com*

SPASA advances aerial imaging capabilities

Vexcel Imaging has announced that Servicios Politécnicos Aéreos (SPASA), an international reference in geospatial solutions with a consolidated presence across Europe, has expanded its aerial mapping capabilities with the acquisition of the UltraCam Osprey 4.2 nadir and oblique aerial camera system. *vexcel-imaging.com*

Mapping and updation of key waterways charts of Indonesia and Philippines

Japan will begin developing high-precision nautical charts for five strategically important waterways across Southeast Asia as part of a broader effort to safeguard maritime trade and reduce dependence on traditional shipping corridors. The project will focus on the Molucca Passage and Ombai Strait in eastern Indonesia, the Sunda Strait in western Indonesia, and the Surigao and Balabac Straits in the Philippines. Each survey will cover roughly 100 square kilometres and include hydrographic mapping, seabed studies and the installation of navigational aids.

Japan's Foreign Ministry will carry out the work in partnership with Indonesia, the Philippines and Timor-Leste (East Timor), with the resulting charts expected to be published by the coastal states. The move comes weeks after tensions in the Middle East renewed concerns over the vulnerability of maritime chokepoints. *https://stratnewsglobal.com*

Amrita Vishwa Vidyapeetham and GSI Sign MoU

Amrita Vishwa Vidyapeetham has signed a Memorandum of Understanding (MoU) with the Geological Survey of India (GSI), Ministry of Mines, Government of India, marking the beginning of a strategic partnership to strengthen collaboration in geosciences, disaster resilience, technological innovation, and landslide risk reduction.

By bringing together GSI's extensive geoscientific expertise and Amrita's strengths in artificial intelligence, IoT, remote sensing, digital technologies, and landslide early warning systems, the partnership aims to develop innovative, science-based solutions for geohazard assessment, monitoring, and disaster risk reduction. The collaboration holds particular significance for strengthening India's efforts in landslide risk reduction. Both institutions are internationally recognised contributors to the International Programme on Landslides (IPL), with Amrita serving as a World Centre of Excellence on Landslide Risk Reduction and GSI playing a leading role in geological investigations, hazard zonation, and geoscientific research. *www.amrita.edu*

Trinidad & Tobago technical bilateral with India

The Survey of India had the first virtual bilateral meeting between India and the Republic of Trinidad & Tobago on 22 July 2026 to explore opportunities for collaboration in drone-based surveying and mapping. The meeting highlighted India's geospatial initiatives, including the NAKSHA Programme, Bharat Land Stack, and the SVAMITVA Scheme, while exploring opportunities for technical cooperation, knowledge sharing, institutional partnerships, and capacity building. The discussions reaffirmed the shared commitment of both nations to advancing geospatial innovation and strengthening bilateral cooperation in modern land surveying and administration.

Nepal, India to Hold Key Border Technical Talks

Nepal and India is likely to hold the 13th meeting of the Survey Officials Committee (SOC) in Lucknow, India, from August 12 to 14 to deliberate on technical issues. The meeting is expected to approve the work plan and budget required for implementing the decisions taken during the seventh meeting of the Boundary Working Group (BWG).

During the seventh BWG meeting, held on July 30 last year, both countries agreed to complete the construction of new border pillars, jointly repair damaged pillars, and undertake other technical works within the next three years.

According to Nepal's Department of Survey, the Lucknow meeting will also review progress on upgrading Global Positioning System (GPS) base stations along the border. *https://english.hindusthansamachar.in*

Focal Point and STMicroelectronics partnership

FocalPoint, UK has entered into a commercial agreement with STMicroelectronics. Both the companies have now advanced their joint S-GNSS® Auto and Teseo solution to a full commercial offering. The joint industry-leading solution is delivered as a simple firmware upgrade to Teseo devices. *focalpointpositioning.com*

NautelNav participates in deployable eLoran concept

NautelNav has announced its participation in a new concept for a field-deployable eLoran station. It could result in the procurement of a number of operational systems for multiple defence organizations worldwide. A deployable eLoran station enables quick replacement of PNT (Position, Navigation, and Timing) systems, such as GPS, that may be jammed or spoofed by hostile entities. Temporary, rapidly deployable eLoran systems, each with a collapsible/portable antenna, are much more difficult to jam and can help ensure mission success in a battlefield arena. Nautel global partner UrsaNav® is teaming with QinetiQ, Roke, and GMV to develop the concept. *https://nautelnav.com*

Boosting navigation for French army vehicles

Eviden and Thales have announced the integration of Thales' Galileo PRS capability into Eviden's P3TS military satellite navigation receiver, used by the French army. It strengthens the resilience of the army's vehicle positioning system by improving its resistance to electronic warfare threats, including jamming and spoofing, while ensuring the integrity and security of positioning data in highly contested operational environments. The solution will be available in two configurations. The first integrates the TopStar Galileo PRS Core Module, providing access to Galileo PRS signals alongside Galileo and GPS open-service signals. The second combines either GPS or the TopStar Smart Receiver, adding advanced anti-jamming capabilities to the later. *www.thalesgroup.com*

Teledyne releases ITAR-free Boson® SX8

Teledyne FLIR OEM has released the ITAR-free Boson® SX8, the first NDAA-compliant, volume production, uncooled longwave infrared (LWIR) thermal camera module to combine an 8-micron pixel pitch with SXGA (1280 × 1024) resolution. The 8-micron pixel enables industry-best thermal performance and four times the resolution of today's high-volume, uncooled VGA (640 × 512) thermal camera modules, all within a similarly sized compact package. *oem.flir.com*

Tersus GNSS launches AG993 modular autosteer kit

Tersus GNSS has launched the AG993, a modular autosteer retrofit kit for agricultural vehicles that combines high-precision GNSS positioning with the company's proprietary Tersus Advanced Positioning satellite correction service and conventional RTK support. *www.tersus-gnss.com*

Furuno Introduces GF-100 GNSS Oscillators

Furuno plans to launch its GF-100 Series of dual-band GNSS disciplined oscillators (GNSSDOs) in November 2026, adding new timing modules designed to improve resilience against GNSS interference in critical infrastructure applications. *www.furuno.com*

SBG Systems launches Pulse-40 OEM IMU

SBG Systems has launched the Pulse-40 OEM, the latest generation of its miniature tactical-grade inertial measurement unit (IMU). Built on the original Pulse-40, the new model delivers improvements in performance, environmental robustness, manufacturing scalability and vibration spectrum monitoring while preserving the compact size, low weight, ultra-low power consumption and integration capabilities of its predecessor. The new Pulse-40 OEM maintains full form and function compatibility with existing Pulse-40 integrations, allowing customers to upgrade to the latest generation with minimal system redesign.

The new version retains the core characteristics of the original, including dimensions of 30×28×13.3 mm, a weight of 19 g, and typical power consumption of 0.3 W. It also preserves tactical-grade inertial performance in an OEM form factor, ultra-low-noise MEMS sensing, continuous built-in test capabilities, a redundant sensor cluster architecture, data output rates up to 2 kHz, and advanced synchronization capabilities. *www.sbg-systems.com*

Safran Electronics & Defense Introduces MEMS Accelerometers

Safran Electronics & Defense has released the MS500 Series, MEMS accelerometers designed for defense and industrial markets requiring precise and reliable inertial sensing. It has developed an ITAR-free solution that combines tactical-grade performance, 200 µg RMS precision over the full

SUBSCRIPTION FORM

YES! I want my Coordinates

I would like to subscribe for (tick one)

☐ 1 year — 12 issues — Rs.2400/US$200

☐ 2 years — 24 issues — Rs.4500/US$350

Postage and handling charges extra.

First name ....

Last name ....

Designation ....

Organization ....

Address ....

....

City .... Pincode ....

State .... Country ....

Phone ....

Fax ....

Email ....

I enclose cheque no. ....

drawn on ....

date .... towards subscription

charges for Coordinates magazine

in favour of **'Coordinates Media Pvt. Ltd.'**

Sign .... Date ....

Mail this form with payment to:

Coordinates
A 002, Mansara Apartments
C 9, Vasundhara Enclave
Delhi 110 096, India.

If you'd like an invoice before sending your payment, you may either send us this completed subscription form or send us a request for an invoice at iwant@mycoordinates.org

MARK YOUR CALENDAR

September 2026

Esri India User Conference
2 - 3 September 2026
New Delhi, India
www.esri.in

ION GNSS+ 2026
14 - 18 September
Orlando, Florida, USA
www.ion.org

Intergeo 2026
15 - 17, September
Munich, Germany
https://dvw.de/intergeo/en

21st International 3D GeoInfo Conference
28 - 29 September
Sofia, Bulagria
https://gdmc.nl/3DCadastres/workshop2026

October 2026

14th International FIG Workshop on the Land Administration Domain Model & 3D Land Administration
1 - 2 October
Sofia, Bulagria
https://gdmc.nl/3DCadastres/workshop2026

ICL-GNSS 2026,
6 - 8 October
Rome, Italy
https://events.tuni.fi

3rd Annual International Geotechnical Innovation Conference
12 - 13 October
Jeddah, Saudi Arabia
https://geotechnicalinnovationconference.com

47th Asian Conference on Remote Sensing
12 - 16 October 2026
New Delhi, India
https://acrs2026.in

November 2026

United Nations World Geospatial Information Congress (3rd UNWGIC)
16 - 19 November
Jeddah, Saudi Arabia
https://ggim.un.org/3UNWGIC

Geoworld
23 - 26 November
Dubai, UAE
https://www.geoworldevent.com

Pacific Islands GIS & Remote Sensing User Conference
30 November - 4 December 2026
Suva, Fiji
https://pgrsc.org

December 2026

IEEE India Geoscience & Remote Sensing Symposium
01 – 04 December 2026, Hyderabad, India
https://ingarss2026.co.in

operating temperature range of -40°C to +85°C, digital output, and optimized SWaP-C for demanding applications. *https://safran-navigation-timing.com*

Pacific Defense wins U.S. Army APNT contract

Pacific Defense has received a contract award from the U.S. Army Program Manager Positioning, Navigation and Timing (PM PNT) for the CMOSS Mounted Form Factor (CMFF) Assured Position, Navigation and Timing (APNT) Block 2 plug-in-card (PIC) development program. It will design, build, and test an enhanced version of its Block 1 APNT PIC aligned to CMFF program requirements, with delivery of initial prototype quantities to support U.S. Army system integration and test activities. *pacific-defense.com*

Rocket Lab's $8 billion Iridium acquisition

Rocket Lab has entered into a definitive agreement to acquire Iridium Communications in an approximately $8 billion cash-and-stock transaction, bringing together launch services, spacecraft manufacturing and one of the world's largest low-Earth orbit (LEO) satellite networks under a single company. *https://rocketlabcorp.com*

EOS introduces Skadi range pole bracket

Eos Positioning Systems has released the Skadi Handle Range Pole Bracket, a new accessory designed to improve field-gear convenience. This accessory is now included with every Skadi 200, Skadi 300 and Skadi Gold GNSS receiver. Designed for compatibility with both the Skadi Smart Handle and Skadi Standard Handle, the new bracket enables users to securely mount their Skadi handle directly to a range pole. It also simplifies the hardware required in the field by eliminating the need for additional hardware when mounting a smartphone or tablet. This integrated configuration makes the Skadi readily available, allowing a quick transition between range-pole and handheld configurations. *https://eos-gnss.com*


No: DL(E)-01/5079/2023-25
Licensed to post without pre-payment U(E) 28/2023-25
Rs.150
Coordinates
Volume XXI, Issue 1, January 2025
Experts Speak:
"Geospatial analytics is becoming more intelligent and powerful"
"GIS users can expect faster, more accurate results and improved field productivity"
Analysis of the cooling effects of urban green spaces in mitigating micro-climate change using geospatial techniques
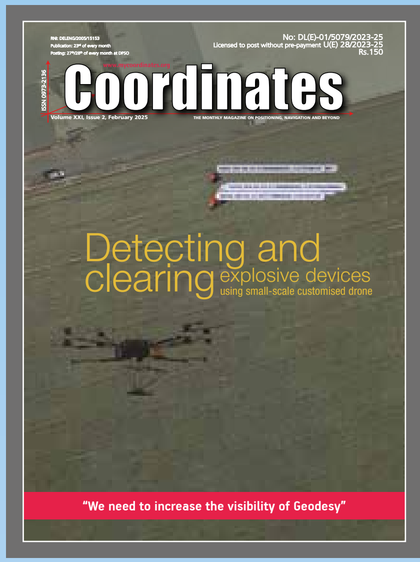
No: DL(E)-01/5079/2023-25
Licensed to post without pre-payment U(E) 28/2023-25
Rs.150
Coordinates
Volume XXI, Issue 2, February 2025
Detecting and clearing explosive devices
using small-scale customised drone
"We need to increase the visibility of Geodesy"
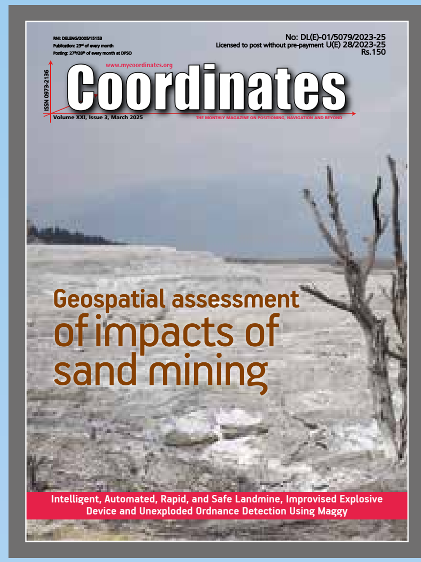
No: DL(E)-01/5079/2023-25
Licensed to post without pre-payment U(E) 28/2023-25
Rs.150
Coordinates
Volume XXI, Issue 3, March 2025
Geospatial assessment of impacts of sand mining
Intelligent, Automated, Rapid, and Safe Landmine, Improvised Explosive Device and Unexploded Ordnance Detection Using Maggy
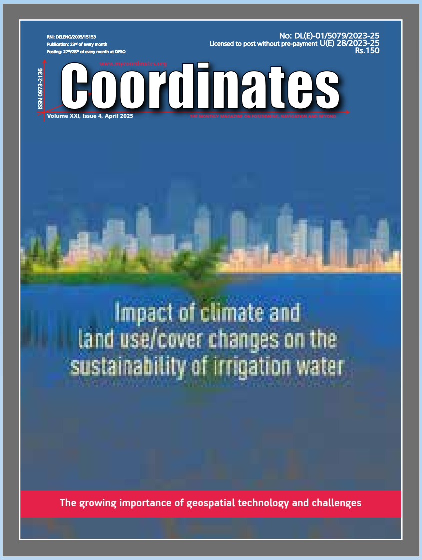
No: DL(E)-01/5079/2023-25
Licensed to post without pre-payment U(E) 28/2023-25
Rs.150
Coordinates
Volume XXI, Issue 4, April 2025
Impact of climate and land use/cover changes on the sustainability of irrigation water
The growing importance of geospatial technology and challenges
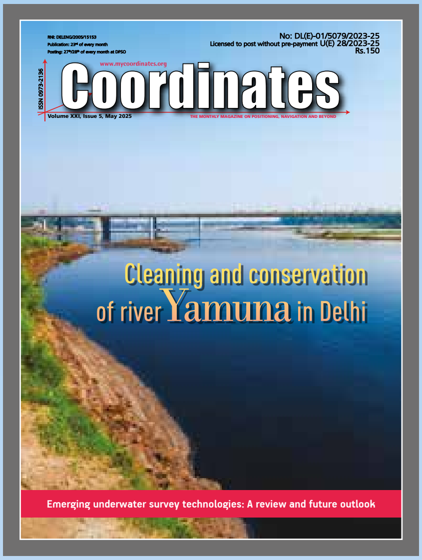
No: DL(E)-01/5079/2023-25
Licensed to post without pre-payment U(E) 28/2023-25
Rs.150
Coordinates
Volume XXI, Issue 5, May 2025
Cleaning and conservation of river Yamuna in Delhi
Emerging underwater survey technologies: A review and future outlook

No: DL(E)-01/5079/2023-25
Licensed to post without pre-payment U(E) 28/2023-25
Rs.150
Coordinates
Volume XXI, Issue 6, June 2025
In this issue
gSim – Low Cost Dual Frequency GPS & Galileo Simulator
GNSS Constellation Specific Monthly Analysis Summary: May 2025
Combating Air Pollution in NCT of Delhi: Strategic Pathways

No: DL(E)-01/5079/2023-25
Licensed to post without pre-payment U(E) 28/2023-25
Rs.150
Coordinates
Volume XXI, Issue 7, July 2025
BEAUTIMETER
Harnessing GPT for assessing architectural and urban beauty based on the 15 properties of living structure
Emerging technologies and their integration in surveying profession
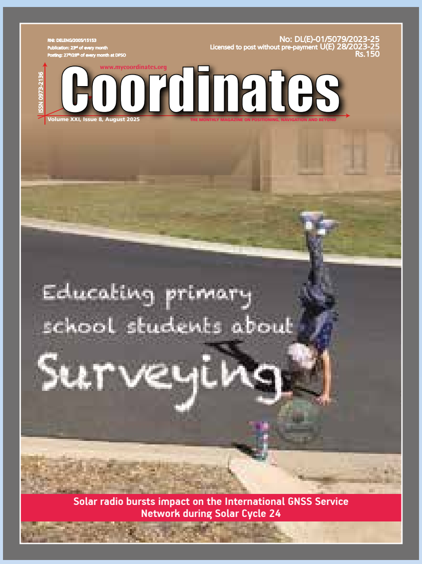
No: DL(E)-01/5079/2023-25
Licensed to post without pre-payment U(E) 28/2023-25
Rs.150
Coordinates
Volume XXI, Issue 8, August 2025
Educating primary school students about Surveying
Solar radio bursts impact on the International GNSS Service Network during Solar Cycle 24
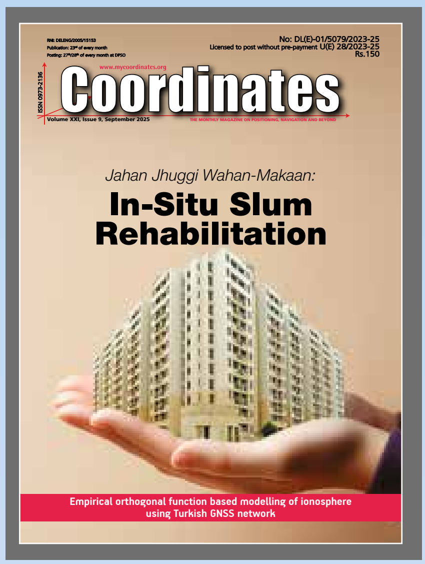
No: DL(E)-01/5079/2023-25
Licensed to post without pre-payment U(E) 28/2023-25
Rs.150
Coordinates
Volume XXI, Issue 9, September 2025
Jahan Jhuggi Wahan-Makaan:
In-Situ Slum Rehabilitation
Empirical orthogonal function based modelling of ionosphere using Turkish GNSS network